# Original Article

# The oxidative modification of transcription factor FOXM1 by Peroxiredoxin1 facilitates DNA damage repair and cancer progression

Ziqing Li<sup>1</sup>, Guixiang Tan<sup>1,2</sup>, Shasha Wu<sup>1</sup>, Hao Guo<sup>1</sup>, Chaozhu Pei<sup>1</sup>, Ziwu Xu<sup>1</sup>, Yan Chen<sup>1</sup>, Li Yu<sup>1</sup>, Mingmin Huang<sup>1</sup>, Yongjun Tan<sup>1</sup>

<sup>1</sup>State Key Laboratory of Chemo/Biosensing and Chemometrics, College of Biology, Hunan Research Center of The Basic Discipline for Cell Signaling, Hunan Engineering Research Center for Anticancer Targeted Protein Pharmaceuticals, Hunan University, Changsha 410082, Hunan, China; <sup>2</sup>Hunan Yuanpin Cell Biotechnology Co., Ltd., Changsha 410000, Hunan, China

Received April 22, 2025; Accepted October 16, 2025; Epub October 25, 2025; Published October 30, 2025

**Abstract:** The oxidative modification of proteins induced by hydrogen peroxide  $(H_2O_2)$  results in the formation of disulfide bond between two cysteines and affects protein conformation and biological function. Transcription factor FOXM1 participates in the development and progression of cancers and its levels are upregulated by the oxidative stress of  $H_2O_2$ -treated condition. In this study, we found that Peroxiredoxin-1 (PRDX1), one of the most  $H_2O_2$ -reactive antioxidant enzymes, interacted with FOXM1 and led to its oxidation under  $H_2O_2$  stimulation through generating an intermolecular disulfide bond with FOXM1 C539, which was subsequently transferred to form an intramolecular disulfide bond between C167 and C175 in the oxidized FOXM1. The PRDX1-mediated oxidative modification enhanced the protein stability and transcriptional activity of FOXM1, which stimulated the transcription of FOXM1 target gene X-ray cross-complementing protein 1 (XRCC1) and improved the repair of  $H_2O_2$ -induced DNA damage in cancer cells. The disruption of PRDX1-mediated FOXM1 oxidation impaired the colony formation ability of cancer cells *in vitro* and the growth and DNA damage repair ability of cancer cells *in vivo*. The analysis of The Cancer Genome Atlas (TCGA) breast cancer patient data confirmed that PRDX1 and FOXM1 together facilitated clinical cancer progression. Overall, we established an  $H_2O_2$ -PRDX1-FOXM1 oxidation pathway that likely contribute to the development and progression of cancers.

**Keywords:** Transcription factor FOXM1, peroxiredoxin-1, oxidative modification of proteins, DNA damage repair, cancer progression

#### Introduction

Reactive oxygen species (ROS) describes the oxygen-derived molecule that has strong reactive ability and contributes physiologically to cell proliferation, differentiation, and migration [1]. If they are beyond physiological levels, ROS will cause oxidative stress that results in a series of consequences such as DNA damage in cells [2, 3], at extreme situations leading to apoptosis [4]. After cells are attacked by ROS, DNA repair pathway is usually activated to repair the damages [5, 6]. Hydrogen peroxide  $(H_2O_2)$  belongs to the ROS chemical family and is not nearly as reactive as other members such as superoxide, singlet oxygen, and hydroxyl radical [7, 8]. To avoid the severe conse-

quence of high  ${\rm H_2O_2}$  levels, antioxidant enzymes participate in clearing  ${\rm H_2O_2}$  in cells [9]. Among them, a family of Peroxiredoxins (PRDXs) plays a critical role for doing so [10]. For example, as a typical 2-Cys PRDX locating in both cytoplasm and nucleus [11], PRDX1 can be oxidized by  ${\rm H_2O_2}$  and then the disulfide bond is generated to form the homodimer of the protein [11]. Subsequently, the oxidized PRDX1 homodimer can be reduced by thioredoxin-1 (TRX1) to restore its reduced state [12]. Through the reduction-oxidation (redox) cycle of PRDX1, the oxidative stress can be effectively controlled.

Interestingly, in addition to its classic redox cycle to eliminate  $\rm H_2O_2$ , PRDX1 can transmit the oxidative signal from  $\rm H_2O_2$  to its interacting pro-

teins [13], generating the oxidative modification of its target proteins. Instead of the formation of the oxidized PRDX1 homodimer, H<sub>2</sub>O<sub>2</sub>treated PRDX1 can form the disulfide bond between PRDX1 and its target proteins, resulting in their oxidation and subsequently affecting their functions. For example, as an important category of PRDX1-targeted proteins, transcription factors are regulated by the oxidative modification and multiple characteristics of transcription factors are altered, such as stability, cellular location, DNA binding and transcriptional activities, and protein-protein interaction [14]. It is reported that PRDX1 is highly expressed in many types of cancer, such as breast cancer and non-small cell lung cancer [15]. Through oxidizing certain transcription factors, PRDX1 contributes to the development and progression of cancers by promoting the proliferation and invasion of cancer cells [16, 17].

FOXM1 belongs to the forkhead transcription factor family, which contains more than 50 members that share the conserved forkhead DNA binding domain [18]. FOXM1 participates in the development and progression of cancers, such as breast cancer and lung cancer [19, 20]. As an important oncogene [21], FOXM1 has been found to stimulate proliferation [22], epithelial-mesenchymal transition (EMT) [23], stemness [24], and prevent senescence [25] in cancer cells. Recently, FOXM1 was reported to function in maintaining ROS homeostasis. FOXM1 was upregulated by H<sub>2</sub>O<sub>2</sub> treatment and subsequently it could stimulate the transcription of several ROS-scavenger genes [26]. Interestingly, FOXM1 was also found to participate in DNA damage repair through directly stimulating the transcription of DNA repair genes such as X-ray cross-complementing protein 1 (XRCC1) [27]. Because XR-CC1 was an essential component for base excision repair and was activated to repair H<sub>2</sub>O<sub>2</sub>caused DNA damage [28], we hypothesized that FOXM1 mediated the process between H<sub>2</sub>O<sub>2</sub> signals and DNA damage repair machinery in cancer cells.

Although the activities of FOXM1 are stimulated by  $\rm H_2O_2$ , whether FOXM1 is oxidatively modified by  $\rm H_2O_2$  and the mechanisms of FOXM1 oxidative modification remain unknown. In this study, we demonstrated that FOXM1 interacted with PRDX1.  $\rm H_2O_2$  induced PRDX1 to form the

disulfide bond between PRDX1 and FOXM1, leading to the oxidation of FOXM1. We identified that PRDX1 generated an intermolecular disulfide bond with FOXM1 C539, which was subsequently transferred to form an intramolecular disulfide bond between C167 and C175 in the oxidized FOXM1. The PRDX1-mediated oxidative modification enhanced the protein stability and transcriptional activity of FOXM1. evidenced by the elevated transcription of FOXM1 target gene XRCC1, and consequently facilitated cells to decrease DNA damage induced by H<sub>2</sub>O<sub>2</sub>. The disruption of PRDX1-mediated FOXM1 oxidation impaired the colony formation ability of cancer cells in vitro and the growth and DNA damage repair ability of cancer cells in vivo. Together, this finding revealed a new post-translational modification of FOXM1 that likely contribute to the development and progression of cancers.

#### Materials and methods

#### Cell culture

Human cell lines MDA-MB-231 and HEK293T cells were purchased from ATCC (Manassas). All cells were cultured in DMEM medium (SIGMA) containing 10% fetal bovine serum (Biological Industries).

# Bioinformatics analysis

To analyze the survival curve of single factor FOXM1 or PRDX1, the Kaplan-Meier curves were downloaded from Kmplot website (https:// kmplot.com/analysis) according to the mRNA expression from gene chip data. The data of clinical breast cancer patients (n=1214) was downloaded from TCGA database. The analysis of gene expression correlation was executed by using 'ggstatsplot' package through R project. To analyze the PRDX1-related survival curve in breast cancer patient subgroups, the mean value of FOXM1 level in breast cancer patients was set as the cut-off value to separate breast cancer patients as FOXM1-High subgroup (n= 654) and FOXM1-Low subgroup (n=560). The mean value of PRDX1 level was set as the cutoff value for separating PRDX1 high or low expression. PRDX1-related survival of patients was calculated by using 'survminer' package at first, and then calculated by using 'survival' package, and the Kaplan-Meier curves were drawn by using 'ggplot2' package by R project.

# Construction of plasmids

The cDNA of full-length FOXM1 (Gene ID: 2305) was amplified from pCMV-Flag-FOXM1 plasmid [29] with primers containing Xhol and Kpnl restriction sites (S: 5'-CCG CTC GAG ATG AAA ACT AGC CCC CGT CGG CCA CT-3' and AS: 5'-CGG GGT ACC CTA CTG TAG CTC AGG AAT AAA CTG GGA-3') and ligated into pLVX-Puro ve ctor (Clontech) or pcDNA3.1 vector (Invitrogen) to obtain pLv-CMV-FOXM1, pCMV-V5-FOXM1 or pCMV-AVI-FOXM1. The truncated FOXM1 (1-224aa) was amplified with primers containing Xhol and Kpnl restriction sites (S: 5'-CCG CTC GAG ATG AAA ACT AGC CCC CGT CGG CCA CT-3' and AS: 5'-CGG GGT ACC CTA TGG TCT GAA GGC TCC TC-3'), and the truncated FOXM1 (1-353aa) was amplified with primers containing Xhol and Kpnl restriction sites (S: 5'-CCG CTC GAG ATG AAA ACT AGC CCC CGT CGG CCA CT-3' and AS: 5'-CGG GGT ACC CTA TGG CTT CAT CTT CCG CCG T-3') and ligated into pc-DNA3.1 vector to obtain pCMV-AVI-FOXM1 (1-224aa) and pCMV-AVI-FOXM1 (1-353aa). The cDNA of PRDX1 (Gene ID: 5052) was amplified from cDNAs of HEK293T cells with primers containing Xbal and EcoRI restriction sites (S: 5'-TGC TCT AGA ATG TCT TCA GGA AAT GCT AA-3' and AS: 5'-CGG AAT TCC TTC TGC TTG GAG AAA T-3') and ligated into pcDNA3.1 vector to obtain pCMV-PRDX1 and pCMV-PRDX1-GFP. The cDNA of TRX1 (Gene ID: 7295) was amplified from cDNAs of HEK293T cells with primers containing Xbal and EcoRI restriction sites (S: 5'-TGC TCT AGA ATG GTG AAG CAG ATC GAG-3' and AS: 5'-CCG GAA TTC GAC TAA TTC ATT AAT GGT-3') and ligated into pcDNA3.1 vector to obtain pCMV-TRX1-GFP.

The pCMV-Flag-FOXM1, pCMV-AVI-FOXM1, pC-MV-PRDX1-GFP, pCMV-TRX1-GFP and pLv-CMV-Flag-FOXM1-puro plasmids were used as the template to construct the point mutational FOXM1, PRDX1 or TRX1 plasmids. The sequences of primers were shown in <u>Table S1</u>.

The pLv-PRDX1-shRNA plasmid was designed to target the sequence: CCG CTC TGT GGA TGA GAC TTT GAG ACT AG, and synthesized by GENECHEM company, Shanghai, China. The p6×FOXM1 Binding-LUC, pXRCC1pro (-1kb-+22-bp)-LUC, pLv-CMV-Flag-FOXM1-puro and pEF-BirA plasmids were described previously [27, 30, 31].

# Lentivirus packaging and infection

pLv-U6-shPRDX1, pLv-CMV-FOXM1, pLv-CMV-puro, pLv-CMV-Flag-FOXM1-puro, pLv-CMV-Flag-FOXM1 C539A-puro or pLv-CMV-Flag-FOXM1 C167A/C175A-puro were transfected into HEK-293T cells with psPAX2 (Addgene 12,260; deposited by Didier Trono) and pMD.2G (Addgene 12,259; deposited by Didier Trono) constructs to produce lentivirus. Then lentiviruses were used to infect HEK293T or MDA-MB-231 for 24 h and the infection was repeated once. MDA-MB-231 cell lines were treated with 1  $\mu g/ml$  puromycin for 72 h to select cells.

# Protein extraction and western blotting

Cells were lysed with 1% Triton X-100/TBS (50 mM Tris, 150 mM NaCl, pH 7.4) containing 0.1% proteases inhibitor (Roche, 05892791001) for 30 min. To collect cytoplasmic and nuclear proteins, cells were lysed in CE buffer (10 mM HEPES pH7.9, 1.5 mM Mgcl, 10 mM KCl, containing protease inhibitor). After centrifugation, the supernatant was collected as cytoplasmic proteins. Then the pellet was resuspended in NE buffer (20 nM HEPES pH7.9, 1.5 mM Mgcl, 0.42 M Nacl, 0.2 mM EDTA, 25% glycerol, containing protease inhibitors). After centrifugation, the supernatant was collected as nuclear proteins. The protein concentration of cell lysates was quantified using a BCA Protein Assay kit (Thermo Fisher Scientific, A65453).

Protein samples were separated by SDS-PAGE gel electrophoresis and transferred to 0.22 μm PVDF membranes (Merck Millipore). Then membranes were analyzed by Western blotting with certain antibodies and imaged by Kodak 4000 MM Imaging System (Kodak) using ECL buffer (New Cell & Molecular Biotech, P10300). The following antibodies were used for Western blotting: anti-V5 (Sangong, D191104, 1:2000), anti-FOXM1 (CST, 20459s, 1:2000), anti-PRDX1 (Abcam, Ab41906, 1:10000), anti-GFP (Sangon, D110008, 1:2000), anti-RFP (Bioworlde, MB2015, 1:5000), anti-Flag (Proteintech, 20543-1-AP, 1:5000), anti-yH2AX (Abcam, Ab81299, 1:10000), anti-TRX1 (Abcam, Ab133-524, 1:10000), anti-Streptavidin (Byotime, A0-305, 1:2000), anti-β-actin (Bioworlde, BS6007-MH, 1:50000), anti-Lamin A/C (Sangong, AG-2517, 1:2000), HRP labeled anti-Rabbit IgG (Beyotime, A0208, 1:2000), HRP labeled anti-Mouse IgG (Proteintech, SA00001-1, 1:5000),

anti-IgG (CST, 2729s). The relative protein levels of FOXM1 or  $\gamma$ H2AX were calculated using Image J software and normalized to the relative protein levels of  $\beta$ -actin (n=3), the curve was graphed with GraphPad Prism 10.

#### Co-immunoprecipitation

Briefly, cell lysates (500 µg) were incubated with anti-V5 antibody (Sangong, D191104) plus Protein A/G PLUS-Agarose beads (SantaCruz, sc-2003), Streptavidin Sepharose beads (SA beads, GE Healthcare, 17-5113-01) or anti-Flag affinity gel (Selleck, B23102). After incubation and washing, proteins on beads were denatured with 1× loading buffer for Western blotting, or eluted using elution buffer (0.1 M Glycine, 0.1% Triton X-100, pH 2.5) for MS.

# Mass spectrometry (MS)

To detect the binding proteins of FOXM1, the immunoprecipitated samples were digested by trypsin, and fractionated samples were measured by LTQ Orbitrap Velos Rro (Thermo Fisher Scientific). To detect the oxidative sensitive cysteine residues, the immunoprecipitated samples were separated equally into two groups. One group sample was treated with 50 mM Dithiothreitol (DTT) (Sangon, A620058) for 5 min, the other group sample did not. After that, two samples were tagged with 10 mM lodo-acetic acid (IAA, Sangon, A600723) at 37°C for 30 min and ready for digestion and measure by LTQ Orbitrap Velos Rro (Thermo Fisher Scientific).

#### Immunofluorescence staining

MDA-MB-231 cells or transfected HEK293T cells were fixed by 4% paraformaldehyde. After blocked with 5% FBS, cells were incubated with anti-FOXM1 (Santacruz, sc-271746, 1:250), anti-PRDX1 (Abcam, Ab41906, 1:250), anti-Flag (Proteintech, 20543-1-AP, 1:250) or anti-yH2-AX (Abcam, Ab81299, 1:250) overnight at 4°C, and then incubated with cy3 tagged anti-Rabbit IgG (Beyotime, A0521, 1:250) or Alexa Fluor 488 tagged anti-Mouse IgG (Beyotime, A0423, 1:250) for 1 h. Then cells were stained by Antifade Mounting Medium with DAPI (Beyotime, P0131), and observed by confocal microscopy (OLYMPUS). The Pearson's Correlation Coefficient values of the co-localization of two proteins were calculated by Image J software and graphed with GraphPad Prism 10.

#### RNA interference

The sequence of small interfering RNA (siRNA) targeting PRDX1: 5'-AAA CUC AAC UGC CAA GUG A-3'. The sequence of siRNA targeting FOXM1: 5'-GGA CCA CUU UCC CUA CUU UTT-3'. All primers were synthesized by GenePharma company, Shanghai, China.

# Non-reducing western blotting

Transfected or infected HEK293T<sup>FOXM1-OE</sup> cells were treated with 100  $\mu$ M  $\rm H_2O_2$  for 2 min and then treated with 100 mM  $\it N$ -ethylmaleimide (NEM) (Sigma, E3876) for 5 min. Control cells were further treated with 50 mM DTT for 5 min. Later, cells were lysed using 1% Triton X-100/TBS (50 mM Tris, 150 mM NaCl, pH 7.4) containing 0.1% Protease inhibitors. The cell lysate was denatured with 5× non-reducing loading buffer (250 mM Tris-Hcl, 10% SDS, 0.5% Bromoxylenol Blue, 50% Glycerol, pH 6.8) at 98°C for 10 min and proteins were separated by SDS-PAGE gel electrophoresis.

# Electrophoretic mobility shift assay (EMSA)

The sequence of dsDNA probe: forward strand 5'-FAM-TTT GTT TAT TTG TTT GTT TAT TTG-3'(Hot), reverse strand 5'-CAA ATA AAC AAA CAA ATA AAC AAA-3'. The 100× cold probe which has the same sequence without FAM tag was used as competitive probe in negative control. All probes were synthesized by Sangon company, Shanghai, China. Cell lysates were incubated with FAM tagged FOXM1 binding DNA Probe in binding buffer (10 mM Tris-Cl, 1 mM MgCl<sub>2</sub>, 4% glycerol, 0.5 mM EDTA, 0.5 mM DTT, 50 mM NaCl, pH 7.6) for 30 min. Then samples were separated by native gel in 0.5× TBE buffer and imaged using Kodak 4000 MM Imaging System (Kodak, Excitation wavelength 465 nm, Emission wavelength 535 nm).

#### Luciferase reporter assay

Transfected cells were lysed using Dual-Luciferase Reporter Assay System (Promega, E19-10) according to the manufacturer's instructions, and the luciferase enzyme activities were measured by Dual-Luciferase Assay System (Promega).

# Protein synthesis inhibition assay

Transfected cells were treated with 10  $\mu$ M cycloheximide (CHX) (Selleck, S7418) and 200

 $\mu M H_2 O_2$  for indicated time. Then cell lysates were collected and analyzed by Western blotting.

# Real-time quantitative PCR (qPCR)

Total RNAs in cells were extracted using Trans-Zol Up kit (TransGen Biotech, ET111-01-V2) according to the manufacturer's instructions. RNAs (1 µg) were reverse transcribed into cDNA using Maxima H Minus First Strand cDNA Synthesis Kit with dsDNase (Thermo Fisher Scientific, K1682). The qPCR was performed with 2X SYBR Green qPCR Mix (bimake, B21202) using CFX96 Real-Time System (BIO-RAD). The sequence of primers used in qPCR: FOXM1-S, 5'-TGG ATT GAG GAC CAC TTT C-3' and FOXM1-AS. 5'-CTC TGG ATT CGG TCG TTT-3': PRDX1-S. 5'-ATC TCG TTC AGG GGC CTT TT-3' and PRDX1-AS, 5'-GCA CAC TTC CCC ATG TTT GT-3'; XR-CC1-S, 5'-ACG GAT GAG AAC ACG GAC AGT G-3' and XRCC1-AS, 5'-CGT AAA GAA AGA AGT GCT TGC CC-3': GAPDH-S. 5'-ACC CAG AAG ACT GTG GAT GG and GAPDH-AS, 5'-TGC TGT AGC CAA ATT CGT TG-3'.

# Colony formation assay

MDA-MB-231<sup>control</sup>, MDA-MB-231<sup>FOXM1</sup>, MDA-MB-231<sup>FOXM1</sup> c539A and MDA-MB-231<sup>FOXM1</sup> c167A/C175A cells were seeded in a 6-well plate and cultured for 14 days. Then cells were washed with cold PBS twice, and fixed by 4 % paraformaldehyde. Later, cells were stained with 0.1% crystal violet and photographed.

# Nude mice xenograft model

BALB/C nude mice (female, 4-6 weeks old) were purchased from Hunan Slac Laboratory Animal Company (Changsha, China), and were housed under specific pathogen-free conditions with 23  $\pm$  1°C, 55%  $\pm$  5% humidity and 12 h of light and darkness. MDA-MB-231 Control, MDA-MB-231<sup>FOXM1</sup>. MDA-MB-231<sup>FOXM1</sup> C539A and MDA-MB-231<sup>FOXM1 C167A/C175A</sup> cells were subcutaneously (S.C.) injected into the back of nude mice (10<sup>6</sup> cells/mouse, n=5 per group). After 13 days, the volumes of tumors were recorded every two days. At 31st day, the mice were euthanized by CO<sub>2</sub> inhalation, and tumors were weighted and prepared for the immunohistochemistry. All animal care and experiments were performed as a protocol approved by the Ethics Review Committee, College of Biology,

Hunan University, following institutional animal care and use guidelines approved by the Laboratory Animal Center of Hunan, China (Protocol No. SYXK [Xiang] 2023-0010). The ethics approval report was attached in the Supplementary file.

#### *Immunohistochemistry*

The collected tumor tissues were fixed with 4% paraformaldehyde and embedded in paraffin. After dewaxing, rehydration, antigen retrieval, endogenous peroxidase blockage and nonspecific binding site blocking, the tumor sections on slices were incubated with anti-8-oxodG antibody (Abcam, ab62623, 1:1200), anti-YH2AX (Abcam, Ab81299, 1:200) or anti-Ki-67 (CST, 9129, 1:400) followed by the incubation with HRP labeled anti-mouse antibody (Abcam, ab205719, 1:2000) or HRP labeled anti-rabbit antibody (Abcam, ab205718, 1:2000). The nucleus was stained with hematoxylin. The slices were photographed by microscope (Olympus).

#### Statistical analysis

Data analysis and visualization were performed using Microsoft Excel, ImageJ FIJI software and GraphPad Prism 10 (GraphPad Software Inc.). Two-tailed unpaired Student's t-test was used to conduct comparison between two groups. Two-way analysis of variance (ANOVA) was used to conduct comparison associated with two factors. P < 0.05 was considered statistically significant.

#### Results

#### FOXM1 interacted with PRDX1

We constructed and transfected pCMV-V5-FOXM1 into HEK293T cells and analyzed the immunoprecipitated protein samples from transfected HEK293T cells by Mass Spectrometry (MS) experiment to identify interacting proteins of FOXM1 (Figure S1A; Table S2). Two peptides of PRDX1 were recognized in the MS result, suggesting that PRDX1 was one of the interacting proteins of FOXM1 (Figure S1B). We confirmed the interaction between PRDX1 and FOXM1 by co-immunoprecipitation (co-IP) experiments and found that the PRDX1-FOXM1 interaction was enhanced by H<sub>2</sub>O<sub>2</sub> treatment (Figure 1A). Confocal microscope observations revealed that endogenous FOXM1 and PRDX1

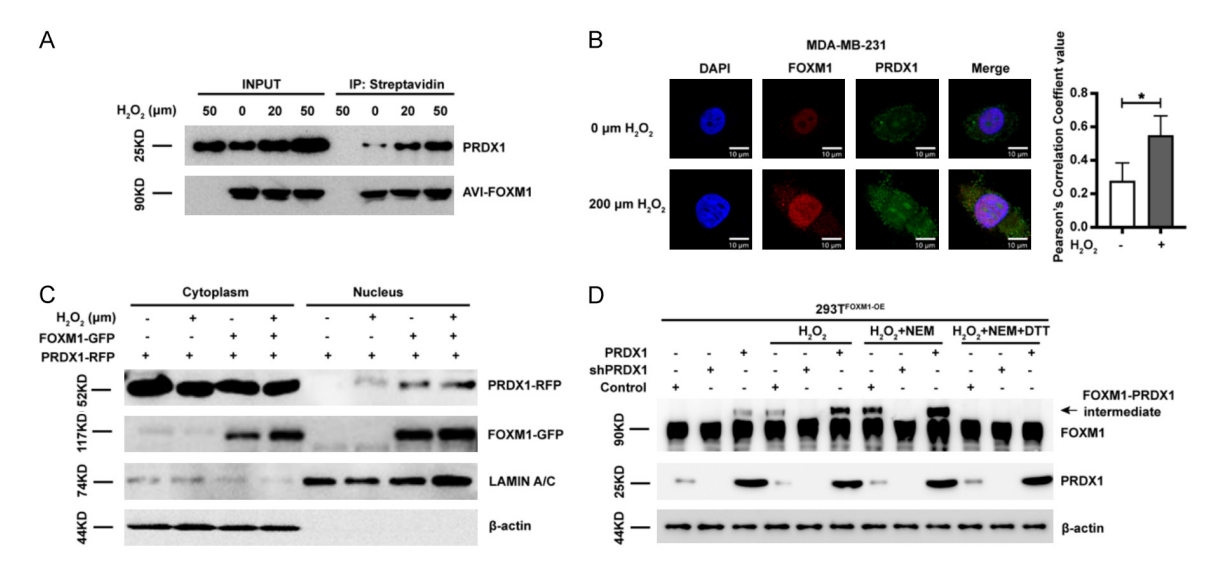


Figure 1. FOXM1 interacted with PRDX1. A. HEK293T cells were transfected with pCMV-AVI-FOXM1 and pEF1-BirA and treated with  $H_2O_2$  (20 μM or 50 μM) for 2 min before harvesting. Before transfection, Biotin were added into cell culture medium. Cell lysates were immunoprecipitated with anti-Streptavidin agarose beads and FOXM1 and PRDX1 proteins were blotted by anti-PRDX1 and anti-Streptavidin antibodies. Ten percent of cell lysates were used as input control. B. MDA-MB-231 cells were treated with or without  $H_2O_2$  (200 μM) for 30 min and immune-stained with anti-FOXM1 and anti-PRDX1 antibodies. The Pearson's Correlation Coefficient values of the co-localization of FOXM1 and PRDX1 were illustrated. n=4, \*, P < 0.05; two-tailed unpaired Student's t-test. Objective, 60×. Scale bars, 10 μm. C. HEK293T cells were transfected with pCMV-FOXM1-GFP and pCMV-PRDX1-RFP, and treated with  $H_2O_2$  (200 μM) for 30 min before harvesting. Then the cytoplasmic and nuclear proteins of cells were harvested separately. The proteins of PRDX1-RFP and FOXM1-GFP were blotted by anti-RFP and anti-GFP antibodies. LAMIN A/C or β-actin was used as the nuclear or cytoplasmic marker, respectively. D. HEK293T<sup>FOXM1-OE</sup> cells were transfected with pCMV-PRDX1 or infected with Lv-U6-shPRDX1. After 24 h, cells were treated with  $H_2O_2$  (100 μM) for 2 min, plus NEM (100 mM, 5 min) treatment. In control group, cell lysates were treated with DTT (100 mM, 5 min). The proteins of FOXM1 and PRDX1 in cell lysates were detected by non-reducing Western blotting with anti-FOXM1 and anti-PRDX1 antibodies. The arrow indicated the intermediate of FOXM1-PRDX1.

were co-localized in nuclei of human breast cancer MDA-MB-231 cells and the co-localization of FOXM1 and PRDX1 was enhanced by  $H_2O_2$  treatment (200  $\mu$ M), evidenced by an increase in Pearson's Correlation coefficient values from 0.28 to 0.55 (Figure 1B). Cytoplasmic and nuclear protein samples from HEK-293T cells overexpressing FOXM1-GFP and PRDX1-RFP also supported the finding that H<sub>2</sub>O<sub>2</sub> stimulated the translocation of PRDX1 from the cytoplasm to the nucleus (Figure 1C). To investigate whether the intermolecular disulfide bond was formed between PRDX1 and FOXM1, protein samples from HEK293T cells stably overexpressing FOXM1 (HEK293TFOXM1-OE) were detected by non-reducing Western blotting, in which the original oxidative status of proteins was maintained [32]. The FOXM1-PRDX1 intermediate, linked by a disulfide bond between PRDX1 and FOXM1, was captured in HEK293TFOXM1-OE cells transfected with pCMV-PRDX1, and the amount of this intermediate was elevated by H2O2 treatment and thiol blocking agent N-ethylmaleimide (NEM) treatment, which prevented the thiol-disulfide exchange reaction [33]. Moreover, this intermediate disappeared in shRNA-mediated PRDX1 knockdown cells, suggesting that PRDX1 mediated the formation of the FOXM1-PRDX1 intermediate. We also found that the reducing reagent Dithiothreitol (DTT) disrupted the formation of the FOXM1-PRDX1 intermediate in the cells (Figure 1D). Together, these results indicated that FOXM1 interacted with PRDX1 in nuclei and the FOXM1-PRDX1 intermediate could be formed through an intermolecular disulfide bond under  $H_2O_2$  stimulation.

The identification of oxidative sensitive cysteines in FOXM1 protein

To identify the specific amino acid in FOXM1 that mediated the formation of the FOXM1-PRDX1 intermediate, we constructed vectors expressing AVI-tagged FOXM1 1-224aa, FOXM1 1-353aa, FOXM1 full-length (1-748aa) and used Streptavidin-Biotin system to immunoprecipi-

tate AVI-FOXM1s in H2O2-treated HEK293T cells. We found that only the full-length FOXM1 (1-748aa) could bind with endogenous PRDX1 while truncated FOXM1 1-224aa or FOXM1 1-353aa could not (Figure 2A), indicating that the 354-748aa region of FOXM1 mediated the binding of FOXM1 to PRDX1. There were only two cysteines (C511 and C539) existing in FOXM1 354 -748aa region (Figure 2B), providing the two potential thiol groups in FO-XM1 responsible for forming an intermolecular disulfide bond between FOXM1 and PRDX1. We expressed FOXM1, FOXM1 C511A, or FO-XM1 C539A in cells and found that the FOXM1 C539A mutation abolished FOXM1-PRDX1 interaction under H<sub>2</sub>O<sub>2</sub> treatment, while the FO-XM1 C511A mutant could interact with PRDX1 (Figure 2C), indicating that FOXM1 C539 mediated the FOXM1-PRDX1 interaction and the following FOXM1 oxidation. The confocal microscope images illustrated that the FOXM1 C539A mutation reduced the co-localization of FOXM1 and PRDX1 (Figure 2D), further supporting that the FOXM1 C539 residue was important for the FOXM1-PRDX1 interaction and the nuclear translocation of PRDX1. It was reported that the intermolecular disulfide bond generated between PRDXs and their targeted proteins was only an intermediate during oxidation and could switch to form an intramolecular disulfide bond in the oxidized proteins [34]. To clarify whether it was the case during FO-XM1 oxidation, we treated the oxidized FOXM1 with Iodoacetic acid (IAA), which could add a modification on the free thiol group (R-SH+ ICH<sub>2</sub>CONH<sub>2</sub>→R-S-CH<sub>2</sub>CONH<sub>2</sub>+HI) and help to distinguish non-oxidized or oxidized cysteines in proteins following DTT treatment [35] (Figure S2A). We performed MS experiments and identified a FOXM1 peptide (164RETCADGEAAGCTI-NNSLSNIQWLR188) containing two newly oxidized cysteines, C167 and C175, because they were not modified by IAA in oxidized condition (NO DTT-treated) but modified in reduced condition (DTT-treated) (Figures 2E and S2B). This demonstrated that once the intermolecular disulfide bond generated between PRDX1 and FOXM1 C539, it was transferred to C167 and C175 to form an intramolecular disulfide bond in the oxidized FOXM1.

PRDX1 enhanced the protein stability and transcriptional activity of FOXM1

The protein levels of FOXM1 were elevated during  $H_2O_2$  treatment [26, 36]. We observed that

the endogenous FOXM1 was upregulated in human breast cancer MDA-MB-231 cells treated with  $H_2O_2$  (200  $\mu$ M) (Figure S3A), while the mRNA levels of FOXM1 were not affected (Figure S3B), suggesting that the elevated FOXM1 protein level was regulated by posttranscriptional modification. To investigate whether PRDX1 affected the protein stability of FOXM1, we treated cells with H<sub>2</sub>O<sub>2</sub> plus protein synthesis inhibitor cycloheximide (CHX) and found that the overexpression of PRDX1 prevented the degradation of FOXM1 protein (Figure 3A). The knockdown of PRDX1 resulted in a rapid degradation of FOXM1 protein compared to the control condition (Figure 3B). In addition, the degradation of the FOXM1 C539A mutant was enhanced compared to that of FOXM1 (Figure 3C), indicating that PRDX1-mediated FOXM1 oxidation contributed to the protein stability of FOXM1 in cells. To test whether the oxidative modification of FOXM1 affected its transcriptional activities, we expressed FO-XM1 or FOXM1 mutants (C160A, C167A, C175A, or C539A) with the p6×F0XM1 Binding-LUC reporter plasmid in cells. FOXM1 C160 is close to the C167A-C175A oxidative modification site but not modified by  $H_2O_2$  signals (see above). Based on the levels of the reporter luciferase expression, all the FOXM1 mutants showed a similar activity as wild type FOXM1 to stimulate the FOXM1-specific promoter under non H<sub>2</sub>O<sub>2</sub>treated condition (Figure 3D), implicating that the point mutations did not impair overall FOXM1 protein folding. The FOXM1 mutants (C167A, C175A, or C539A) exhibited reduced transcriptional activities compared to FOXM1 or FOXM1 C160A mutant under H2O2-treated conditions (Figure 3D), suggesting that the oxidative modification of FOXM1 by PRDX1 contributed to the transcriptional activities of FOXM1. Next, we performed electrophoretic mobility shift assays (EMSAs) with FOXM1 or FOXM1 mutants (C160A, C167A, C175A, or C539A) plus the FAM-labeled DNA probe containing FOXM1 binding sites under H2O2-treated conditions. We found that the FOXM1 C167A, C175A, or C539A mutant could not bind to the DNA probe as effectively as FOXM1 (Figure 3E), implicating that the oxidative modification of FOXM1 by PRDX1 contributed to the DNA binding abilities of FOXM1. Moreover, FOXM1 C160A did not affect the DNA-binding abilities of FOXM1 (Figure 3E), further suggesting that the loss of FOXM1 oxidation resulted in the DNA-

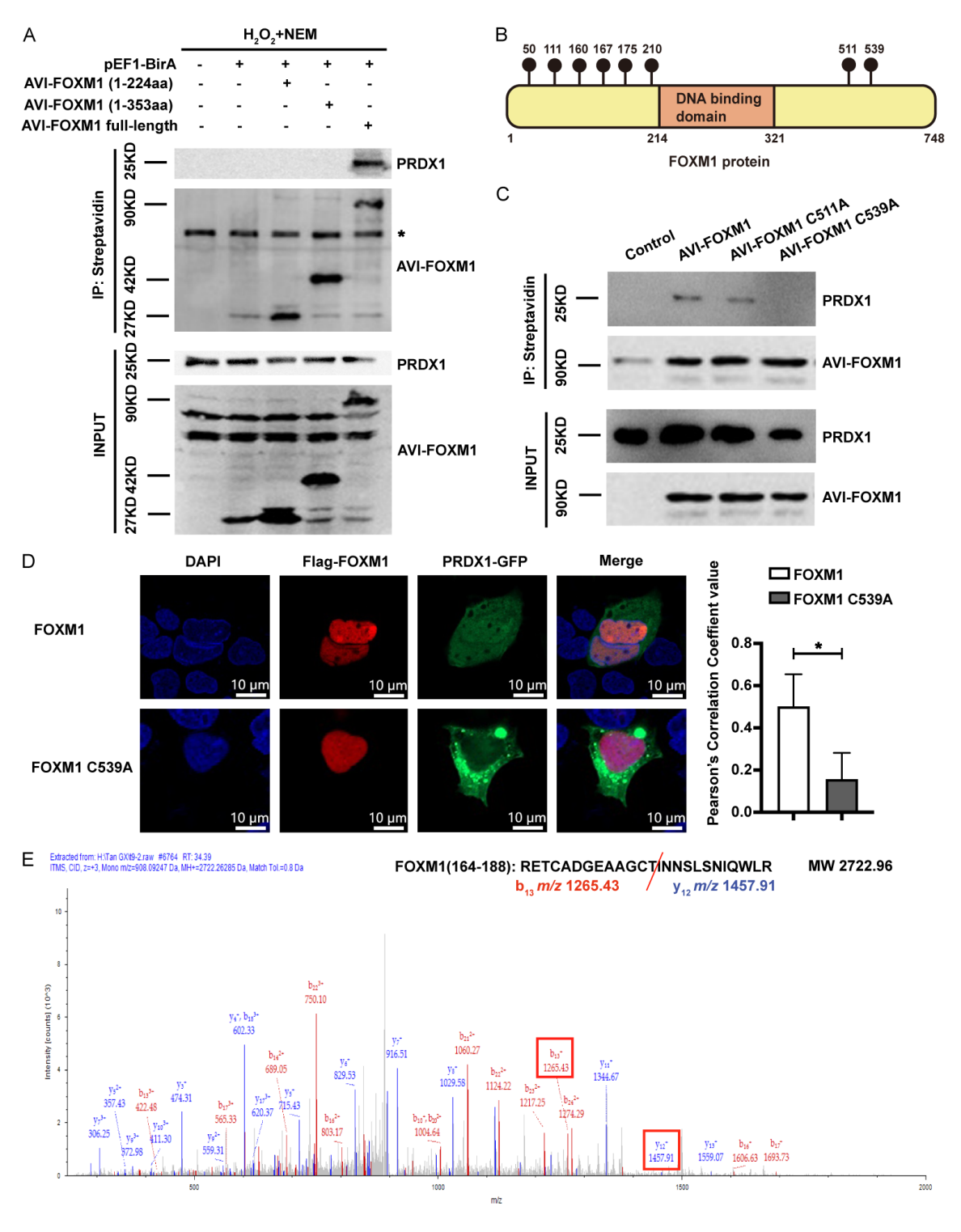
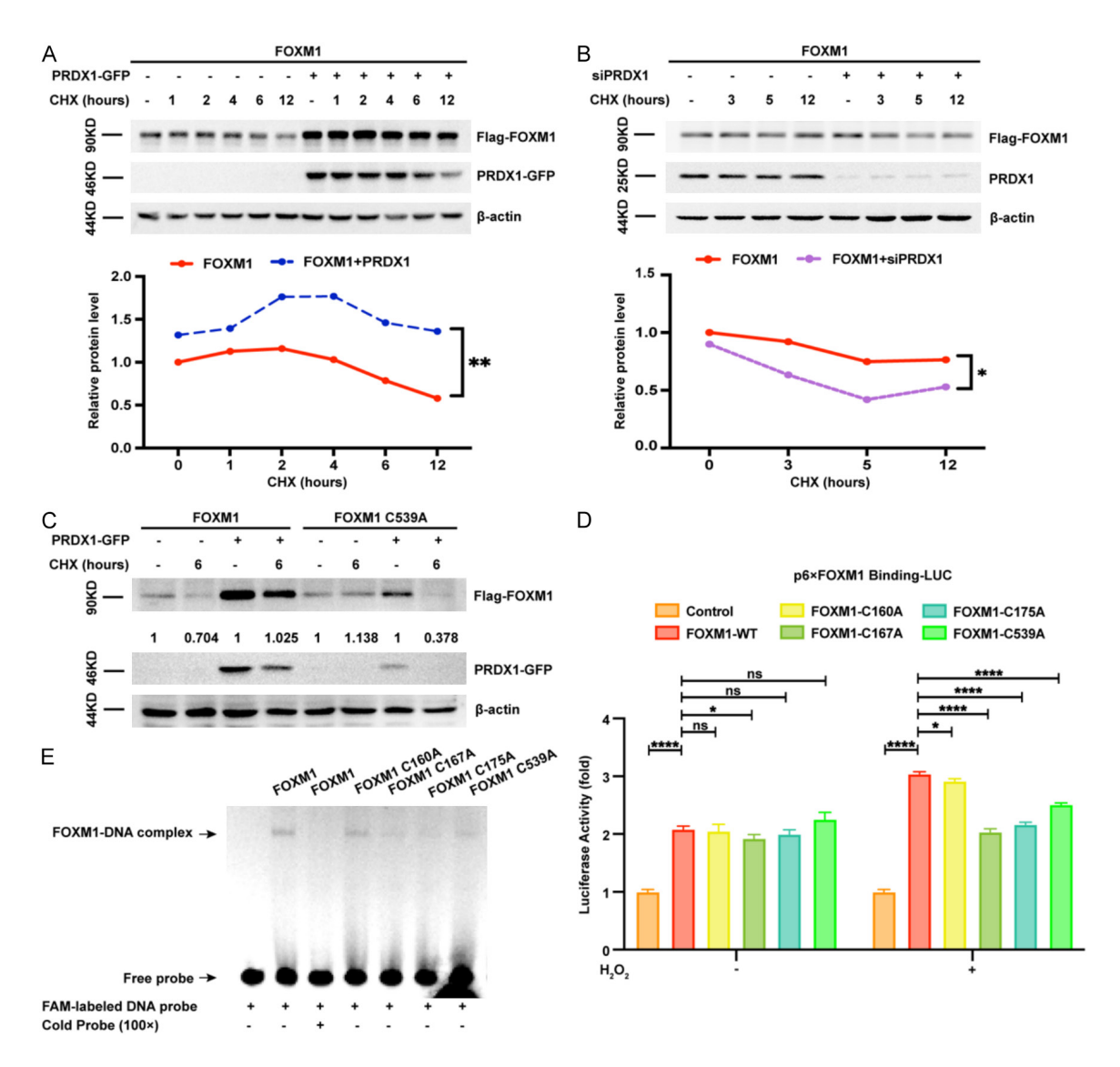


Figure 2. The identification of oxidative sensitive cysteines in FOXM1 protein. A. HEK293T cells were transfected with pCMV-AVI-FOXM1 (1-224aa), pCMV-AVI-FOXM1 (1-353aa), or pCMV-AVI-FOXM1 full-length plus pEF1-BirA and treated with  $\rm H_2O_2$  (100  $\rm \mu M$ ) for 2 min before harvesting. Before transfection, Biotin were added into cell culture medium. Cell lysates were incubated with anti-Streptavidin agarose beads. The proteins of PRDX1 and AVI-FOXM1s were blotted by anti-PRDX1 and anti-Streptavidin antibodies. Ten percent of cell lysates were used as input control. Asterisk indicated non-specific band. B. The schematic of cysteine residues position in FOXM1 protein. C. HEK293T cells were transfected with pCMV-AVI-FOXM1, pCMV-AVI-FOXM1 C511A, or pCMV-AVI-FOXM1 C539A plus pEF1-BirA and treated with  $\rm H_2O_2$  (100  $\rm \mu M$ ) for 2 mins before harvesting. Before transfection, Biotin were added into cell culture medium. Cell lysates were incubated with anti-Streptavidin agarose beads. The proteins of PRDX1 and AVI-FOXM1s

were blotted by anti-PRDX1 and anti-Streptavidin antibodies. Ten percent of cell lysates were used as input control. D. HEK293T cells were transfected with pCMV-Flag-FOXM1 or pCMV-Flag-FOXM1 C539A plus pCMV-PRDX1-GFP, and treated with  $\rm H_2O_2$  (200  $\mu$ M) for 30 min before harvesting. After fixation, cells were immuno-stained with anti-Flag antibodies. The Pearson's Correlation Coefficient values of the co-localization of FOXM1 and PRDX1 were illustrated. n=4, \*, P < 0.05; two-tailed unpaired Student's t-test. Objective, 60×. Scale bars, 10  $\mu$ m. E. The identification of intramolecular disulfide bond in the oxidized FOXM1. Samples were produced as procedures in Figure S2A and the identified FOXM1 peptides from MS were showed in Figure S2B. The spectrum of FOXM1 (164-188) peptide in No DTT group confirmed that FOXM1 C167 and C175 were not modified by IAA.



**Figure 3.** PRDX1 enhanced the protein stability and transcriptional activity of FOXM1. A. HEK293T cells were transfected with pCMV-Flag-FOXM1 and pCMV-PRDX1-GFP and treated with CHX (20 μg/ml) and  $\rm H_2O_2$  (200 μM) by a time gradient (0, 1, 2, 4, 6 or 12 h) before harvesting. The proteins of FOXM1 and PRDX1 in cell lysates were blotted by anti-Flag and anti-GFP antibodies. n=3, \*\*\*, P < 0.01; two-way ANOVA. B. HEK293T cells were transfected with pCMV-Flag-FOXM1 and siPRDX1 for 48 h and treated with CHX (20 μg/ml) and  $\rm H_2O_2$  (200 μM) by a time gradient (0, 3, 5 or 12 h) before harvesting. The proteins of FOXM1 and PRDX1 in cell lysates were blotted by anti-Flag and anti-PRDX1 antibodies. n=3, \*, P < 0.05; two-way ANOVA. C. HEK293T cells were transfected with pCMV-Flag-FOXM1 or pCMV-Flag-FOXM1 C539A, plus pCMV-PRDX1-GFP. Before harvesting, cells were treated with CHX (20 μg/ml) and  $\rm H_2O_2$  (200 μM) for 6 h. The proteins of FOXM1 and PRDX1 in cell lysates were blotted by anti-Flag and anti-GFP antibodies. D. HEK293T cells were transfected with pCMV-Flag-FOXM1 C160A, pCMV-Flag-FOXM1 C167A, pCMV-Flag-FOXM1 C175A, or pCMV-Flag-FOXM1 C539A together with loading control luciferase reporter plasmids pRL-CMV and luciferase reporter plasmids p6×FOXM1 Binding-LUC and treated with or without  $\rm H_2O_2$  (200

# The oxidative modification of FOXM1

 $\mu$ M) for 24 h. Then cell lysates were prepared from these cells and the activities of dual luciferase were measured. n=3 for each group, ns, P > 0.05; \*, P < 0.05; \*\*\*\*, P < 0.0001; two-tailed unpaired Student's t-test. E. The EMSA experiment was performed by cell lysates (10  $\mu$ g) and the FAM-labeled DNA probes (50 nM). HEK293T cells that were transfected with pCMV-Flag-FOXM1, pCMV-Flag-FOXM1 C160A, pCMV-Flag-FOXM1 C167A, pCMV-Flag-FOXM1 C175A, or pCMV-Flag-FOXM1 C539A and treated with H $_2$ O $_2$  (200  $\mu$ M) for 24 h before harvesting. The cold probes without FAM label (100×, 5 mM) were used as competitive probe to show the specificity of FOXM1-DNA complex formation. The upper arrow indicated the FOXM1-DNA complex, and the lower arrow indicated free DNA probes.

binding defect of FOXM1 C167A, C175A, and C539A mutants.

The PRDX1-mediated FOXM1 oxidation participated in DNA damage repair

ROS-induced oxidative stress resulted in DNA damage [2] and both PRDX1 and FOXM1 were found to facilitate DNA damage repair in cells [15, 27]. We also confirmed that the H<sub>2</sub>O<sub>2</sub> treatment could induce DNA damage, evidenced by the increased levels of yH2AX, a marker of DNA damage [37], in cells (Figure S4). To determine whether PRDX1-mediated FOXM1 oxidation correlated with DNA damage repair, we measured the levels of yH2AX in H2O2-treated MDA-MB-231 cells. We found that the knockdown of PRDX1 or FOXM1 resulted in a significant increase of yH2AX levels in the cells (Figure 4A). The overexpression of PRDX1 abolished the upregulation of yH2AX levels in H2O2-treated cells, while PRDX1 C52S/C173S mutant, containing mutations on PRDX1 oxidative catalytic sites C52 and C173 [38], could not do so (Figure 4B), suggesting that the oxidative catalytic function of PRDX1 was needed for preventing DNA damage in cells. Next, we found that the overexpression of wild-type FOXM1 also abolished the upregulation of yH2AX levels in H<sub>o</sub>O<sub>o</sub>-treated cells, while FOXM1 C539A mutant or FOXM1 C167A/C175A mutant could not do so (Figure 4C), suggesting that the oxidation of FOXM1 was needed for preventing DNA damage in cells. The immunostaining of yH2AX further confirmed this result when the signals of yH2AX were compared between non-transfected and transfected cells in the same plate (Figure 4D). FOXM1 was reported to prevent DNA damage by stimulating the transcription of DNA damage repair genes such as XRCC1. As predicted, FOXM1 activated the promoter of XRCC1 in co-transfection experiments and the addition of PRDX1 further enhanced FO-XM1 transcriptional activities on this promoter (Figure 4E), suggesting that PRDX1-mediated FOXM1 oxidation participated in DNA damage

repair. In addition, PRDX1 C52S/C173S mutant or the knockdown of PRDX1 abolished FO-XM1 transcriptional activities on this promoter (Figure 4E). Furthermore, FOXM1 C539A mutant or FOXM1 C167A/C175A mutant was not able to activate the XRCC1 promoter and consequently could not upregulate the endogenous levels of XRCC1 mRNA in cells as much as wild-type FOXM1 (Figure 4F and 4G). Together, these results demonstrated that PR-DX1-oxidized FOXM1 stimulated the expression of DNA damage repair genes such as XRCC1 to prevent ROS-induced DNA damage.

The PRDX1-mediated FOXM1 oxidation facilitated the breast cancer progression

To assess the roles of the PRDX1-mediated FOXM1 oxidation in cancer progression, we generated MDA-MB-231 cell lines stably overexpressing FOXM1, FOXM1 C539A mutant, or FOXM1 C167A/C175A mutant (Figure S5). Colony formation assays showed that MDA-MB-231<sup>FOXM1</sup> cells exhibited an enhanced ability to form cell colonies compared to the control cells, while MDA-MB-231FOXM1 C539A cells or MDA-MB-231<sup>FOXM1 C167A/C175A</sup> exhibited a similar ability of colony formation as the control cells (Figure **5A**), suggesting that the disruption of FOXM1 oxidation impaired the tumorigenesis ability of cancer cells in vitro. Next, we implanted the cells subcutaneously into the backs of BALB/C nude mice to generate xenograft mouse models. The growth curves of engrafted tumors showed that MDA-MB-231FOXM1 cells grew significantly faster than the control cells, while MDA-MB-231 FOXM1 C539A cells or MDA-MB-231<sup>FOXM1</sup> C167A/C175A exhibited a similar growth speed as the control cells (Figure 5B), suggesting that the disruption of FOXM1 oxidation impaired the growth ability of cancer cells in vivo. The engrafted tumors were collected at the end of the experiments and the weight of tumors was measured, further supporting that the disruption of FOXM1 oxidation inhibited the cancer cell proliferation in vivo (Figure 5C). The

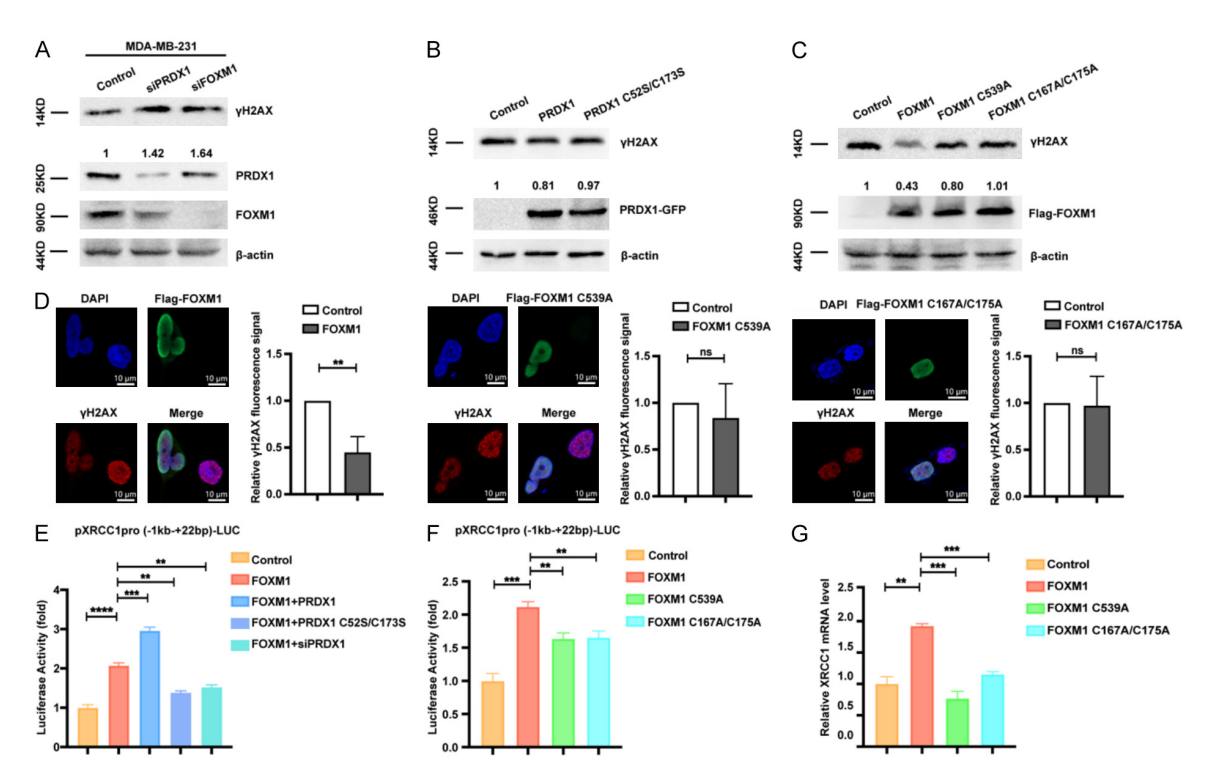
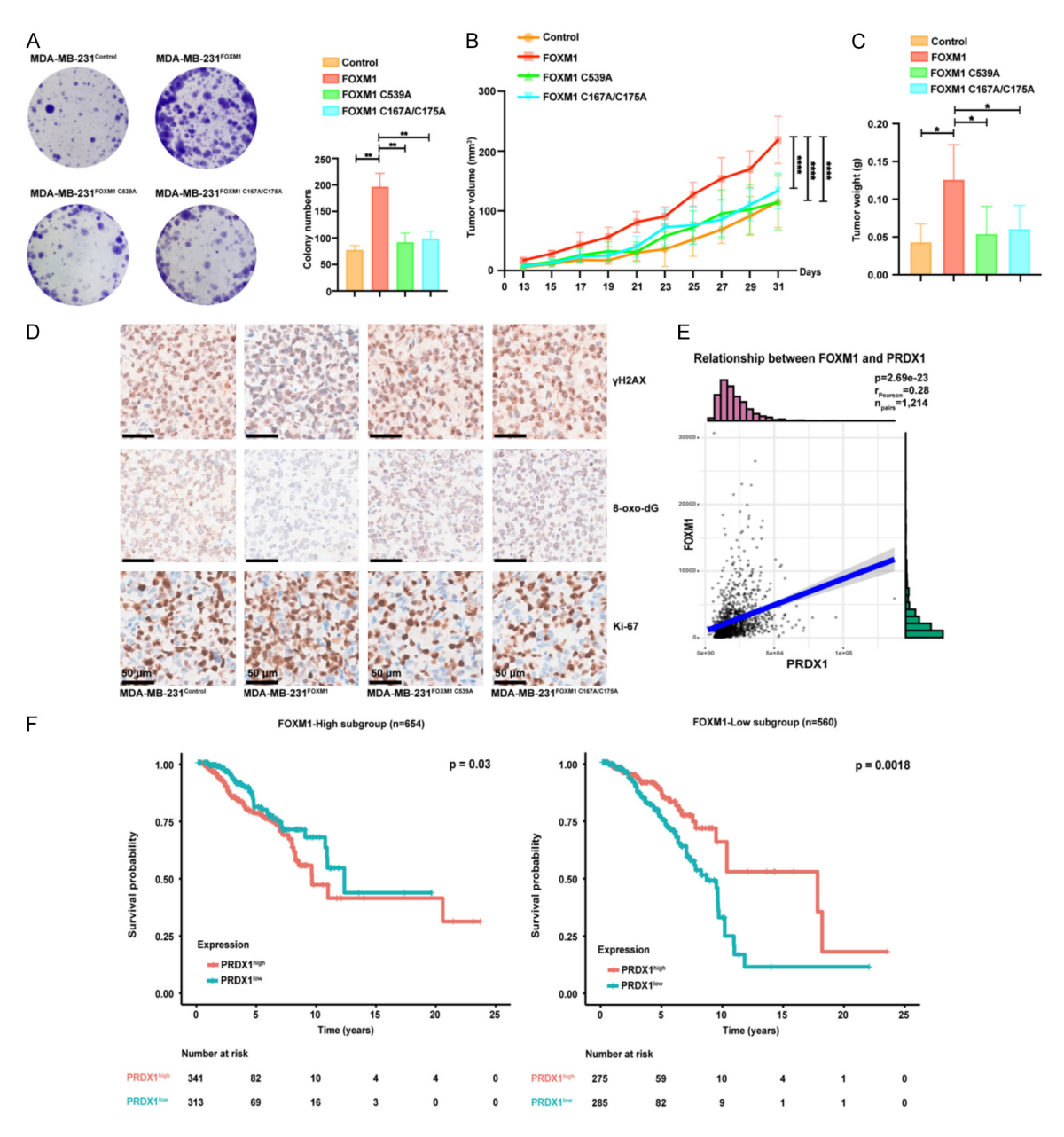


Figure 4. The PRDX1-mediated FOXM1 oxidation participated in DNA damage repair. (A) MDA-MB-231 cells were transfected with siFOXM1 or siPRDX1 and treated with H<sub>2</sub>O<sub>2</sub> (200 µM) for 24 h before harvesting. The proteins of γH2AX, F0XM1 and PRDX1 in cell lysate were blotted by anti-γH2AX, anti-F0XM1 and anti-PRDX1 antibodies. (B) HEK293T cells were transfected with pCMV-PRDX1-GFP or pCMV-PRDX1 C52S/C173S-GFP and treated with H<sub>2</sub>O (200 μM) for 24 h before harvesting. The proteins of γH2AX and PRDX1 in cell lysate were blotted by anti-γH2AX and anti-GFP antibodies. (C) HEK293T cells were transfected with pCMV-Flag-FOXM1, pCMV-Flag-FOXM1 C539A, or pCMV-Flag-FOXM1 C167A/C175A and treated with H<sub>2</sub>O<sub>2</sub> (200 µM) for 24 h before harvesting. The protein levels of γH2AX and FOXM1 in cell lysate were blotted by anti-γH2AX and anti-Flag antibodies. (D) HEK293T cells were transfected with pCMV-Flag-FOXM1, pCMV-Flag-FOXM1 C539A, or pCMV-Flag-FOXM1 C167A/C175A and treated with H<sub>2</sub>O<sub>2</sub> (200 μM) for 24 h before harvesting. After fixation, cells were immuno-stained with anti-γH2AX and anti-FOXM1 antibodies. The immunofluorescence intensities of anti-yH2AX signals were illustrated. n=3, ns, P > 0.05; \*\*, P < 0.01; two-tailed unpaired Student's t-test. Objective, 60×. Scale bars, 10 µm. (E) HEK293T cells were transfected with pCMV-Flag-FOXM1, pCMV-PRDX1-GFP, pCMV-PRDX1 C52S/C173S-GFP, or siPRDX1, together with pRL-CMV and pXRCC1pro(-1kb-+22bp)-LUC and treated with H<sub>2</sub>O<sub>2</sub> (200 μM) for 24 h before harvesting. Cell lysates were collected from cells to measure the dual luciferase activities. (F) HEK293T cells were transfected with pCMV-Flag-FOXM1, pCMV-Flag-FOXM1 C539A, or pCMV-Flag-FOXM1 C167A/C175A, together with pRL-CMV and pXRCC1pro(-1kb-+22bp)-LUC and treated with H<sub>2</sub>O<sub>2</sub> (200 µM) for 24 h before harvesting. Then cell lysates were collected from cells to measure the dual luciferase activities. (G) HEK293T cells were transfected with pCMV-Flag-FOXM1, pCMV-Flag-F0XM1 C539A, or pCMV-Flag-F0XM1 C167A/C175A and treated with H<sub>2</sub>O<sub>2</sub> (200 µM) for 24 h before harvesting. The mRNA levels of XRCC1 were detected by αPCR and normalized to the GAPDH. In (E-G), n=3 for each group. \*\*, P < 0.01; \*\*\*, P < 0.001; \*\*\*\*, P < 0.0001; two-tailed unpaired Student's t-test.

tumor tissue sections were stained with anti-γH2AX, anti-8-oxo-dG, or anti-Ki-67 antibodies, which could quantify the levels of or DNA damage (γH2AX and 8-oxo-dG) [37, 39] or proliferation (Ki-67) [40]. We observed that the tumors from MDA-MB-231<sup>FOXM1</sup> cells possessed much lower γH2AX and 8-oxo-dG signals than that of the control cells, while the tumors from MDA-MB-231<sup>FOXM1</sup> C539A cells or MDA-MB-231<sup>FOXM1</sup> C167A/C175A exhibited similar levels of γH2AX and 8-oxo-dG signals as that of the control cells (**Figure 5D**), suggesting that the dis-

ruption of FOXM1 oxidation impaired its DNA damage repair functions *in vivo*. Moreover, the tumors from MDA-MB-231<sup>FOXM1</sup> cells possessed the highest levels of Ki-67 among four groups (**Figure 5D**), suggesting that the disruption of FOXM1 oxidation impaired cancer cell proliferation *in vivo*. Based on that FOXM1 and PRDX1 were highly expressed in many types of cancers [41-44], we found that the expression levels of FOXM1 and PRDX1 were positively correlated among clinical breast cancer patients from TCGA database (n=1214) (**Figure 5E**). The anal-



**Figure 5.** The PRDX1-mediated FOXM1 oxidation facilitated the breast cancer progression. A. MDA-MB-231<sup>control</sup>, MDA-MB-231<sup>FOXM1</sup>, MDA-MB-231<sup>FOXM1</sup> C167A/C175A cells (400 cells per well) were seeded in 6-well plate and cultured for 14 days. Then cell colonies were photographed, and the numbers of colonies were counted and presented at right graph. \*\*, P < 0.01; two-tailed unpaired Student's t-test. B. The BALB/C nude mice (female, 4-6 weeks old) were subcutaneously (S.C.) injected with MDA-MB-231<sup>control</sup>, MDA-MB-231<sup>FOXM1</sup>, MDA-MB-231<sup>FOXM1</sup> C167A/C175A cells (1×10<sup>6</sup> cells per mouse, n=5 per group) and fed for 31 days. At Day 13 post the injection of cells, the tumor volumes were measured every two days to get the growth curves. Tumor volume (V) was calculated as V= length × width<sup>2</sup> × 1/2. \*\*\*\*, P < 0.0001; Two-way ANOVA. C. At Day 31 post the injection of cells, the tumor weights were measured. n=5 for each group, \*, P < 0.05; two-tailed unpaired Student's t-test. D. The tumor tissue sections of MDA-MB-231<sup>control</sup>, MDA-MB-231<sup>FOXM1</sup>, MDA-MB-231<sup>FOXM1</sup> C167A/C175A</sup> xenograft tumors were immuno-stained with anti-γH2AX, anti-8-oxo-dG and anti-Ki-67 antibodies. Magnification, 40×. Scale bars, 50 μm. E. The gene expression correlation between FOXM1 and PRDX1 in the breast cancer patients (n=1214) was executed by R project. F. The PRDX1-worsened survival in breast cancer patients relied on the high levels of FOXM1 expression. PRDX1-related survival of patients in the FOXM1-High subgroup (n=654) or FOXM1-Low subgroup (n=560) was analyzed by R project.

ysis from Kmplot website (https://kmplot.com/ analysis) showed that the high expression levels of either FOXM1 or PRDX1 were associated with a shorter life span in breast cancer pa-

tients (Figure S6). To test whether PRDX1mediated FOXM1 oxidation facilitating clinical cancer progression, we first separated the breast cancer patients to a FOXM1-High subgroup (n=654) and a FOXM1-Low subgroup (n=560) based on the mean expression level of FOXM1. Then, we analyzed the survival probability according to the levels of PRDX1 within the two subgroups. We found that the high levels of PRDX1 among the FOXM1-High patients (n=341) resulted in a worse survival probability than that of the low levels of PRDX1 among the FOXM1-High patients (n=313) (Figure 5F), indicating that the FOXM1-related poor prognosis among breast cancer patients relied on the high levels of PRDX1. Consistently, we found that the high levels of PRDX1 among the FO-XM1-Low patients (n=275) showed a better survival probability than that of the low levels of PRDX1 among the FOXM1-Low patients (n=285) (Figure 5F), suggesting that the PRDX1-related poor prognosis among breast cancer patients depended on the high levels of FOXM1. These results supported that PRDX1 and FOXM1 worked together in cancer cells and PRDX1mediated FOXM1 oxidation likely contribute to the progression of clinical breast cancers.

#### Discussion

Our results revealed a novel mechanism by which PRDX1 regulated FOXM1 activity under oxidative stress conditions in cancer cells. Specifically, PRDX1 mediated the oxidative modification of FOXM1, leading to its stabilization and subsequent enhancement of its transcriptional activity. This novel post-translational modification of FOXM1 played a crucial role in orchestrating the expression of DNA repair genes such as XRCC1, thereby protecting cells from the deleterious effects of H<sub>2</sub>O<sub>2</sub>. This is the first report providing a mechanism of FOXM1 oxidative modification in response to H<sub>2</sub>O<sub>2</sub>induced stress. Given the enhanced functionality of FOXM1, PRDX1 contributed to FOXM1's oncogenic properties in cancer cells, thereby decreasing the survival rate for breast cancer patients in clinical settings. Our findings provided insights into the molecular mechanisms underlying the regulation of FOXM1 activity by PRDX1 and highlighted the potential implications of this pathway in cancer progression.

The interchange of intramolecular disulfide bond was reported on certain proteins harboring numerous cysteine residues [45, 46]. For example, the C24-C55 disulfide bond within Immunoglobulin27 could interact with the reduced C32 of the protein, thereby generating a novel C32-C24 or C32-C55 disulfide bond in the protein [46, 47]. We believed that this intramolecular disulfide bond-interchange also occurred within FOXM1 protein. The C539 of FO-XM1 served as the binding site for oxidative PRDX1 and a disulfide bond was formed between the two proteins. Subsequently this disulfide bond was transferred to form a new disulfide bond between C167-C175 within FO-XM1, as confirmed through MS analysis. Previous studies demonstrated that the N-terminus of FOXM1 interacted with its C-terminus [48], providing a potential spatial proximity between C539 and C167 or C175, thus facilitating the disulfide bond formation. Oxidative modifications altered both the protein's stability and transcriptional activity of FOXM1, possibly due to the conformational shift triggered by the disulfide bond formation. Nevertheless, due to the uncharacterized full-length FOXM1 protein structure, the precise protein structural alterations caused by FOXM1 oxidation remained elusive. In addition, a stable disulfide bond formed between C539-C167 within FOXM1 likely also existed, based on the prediction of the oxidative modification occurred on C167 alone in MS analysis (Figure S2B). This type of FOXM1 oxidative modification and its biological functions need further study in the future.

The PRDX1-oxidized proteins could be reduced by TRX1 [49]. It's proposed that PRDX1 and TRX1 jointly managed the oxidative-reductive status of a given protein dynamically, thereby impacting the functions of the protein [50-52]. We also identified that TRX1 could interact with FOXM1 via a disulfide bond (Table S2; Figure S7A and S7B), Following the mutation of C167. C175, or C539 within FOXM1, the FOXM1-TRX1 interaction was disrupted (Figure S7A). Additionally, TRX1 diminished the role of FOXM1 in DNA damage repair by suppressing the activation of the XRCC1 promoter (Figure S7C and S7D). Furthermore, the C32S/C35S TRX1 mutant, which lost its reduction activity, failed to regulate FOXM1 in cells (Figure S7C and S7D).

These findings suggested that the oxidative FOXM1 could be reduced by TRX1, indicating the reversibility of the oxidative modification of FOXM1. Notably, the oxidation and reduction of a protein always follow a specific time sequence [33]. It was documented that signal transducer and activator of transcription 3 (STAT3) was oxidized by PRDX2 within 10 seconds post  $\rm H_2O_2$  exposure, subsequently being reduced by TRX1 at 3 minutes and 40 seconds [33]. Hence, it implicated that FOXM1 likely possess a similar reaction order with PRDX1 and TRX1, which regulated the oxidative-reductive status of FOXM1 dynamically (Figure S8).

In addition to PRDX1, the PRDX family encompasses five other members, including PRDX2, PRDX3, PRDX4, PRDX5, and PRDX6 [53]. PR-DX1-4 are typical 2-Cys PRDXs possessing comparable secondary structural features [54]. PRDX5 is an atypical 2-Cys PRDX that normally is monomeric and PRDX6 is a 1-Cys PRDX [34]. Through mass spectrometry analysis of FOXM1interacting proteins, we found that not only PRDX1 but also PRDX2 and PRDX4 could serve as potential interacting partners of FOXM1 (Table S2). Intriguingly, PRDX2 and PRDX4 have been reported to possess an analogous oxidative function to PRDX1 in modifying proteins [33, 55, 56]. Furthermore, PRDX2 typically resides in both the cytoplasm and nucleus, while PRDX4 has been detected within the endoplasmic reticulum [53]. These findings suggested a potential that PRDX2 and PRDX4 likely indeed oxidize FOXM1, which remained to be elucidated in the future.

# Conclusion

We found that  ${\rm H_2O_2}$ -induced PRDX1 formed a disulfide bond with FOXM1 C539, subsequently leading to the formation of a disulfide bond between C167 and C175 in FOXM1, facilitating its protein stability and transcriptional activity. Moreover, the inhibition of FOXM1 oxidative modification through mutation at C167/C175 or C539 abolished the transcription of XRCC1, thereby decreasing the DNA damage repair. The oncogenic properties of FOXM1 were enhanced by PRDX1, diminishing the survival rate for breast cancer patients in clinical settings. These results provided an understanding to develop potential therapeutics for breast can-

cer by targeting PRDX1-mediated FOXM1 oxidation.

# Acknowledgements

This study was supported by grants from the National Natural Science Foundation of China (No. 81773169, No. 31701245), Hunan Science and Technology Innovation Plan (2025ZYJ003), Hunan Natural Science Foundation (2022JJ30184), China Changsha Development and Reform Commission "Mass entrepreneurship and innovation program" (2018-68) and "Innovation platform construction program" (2018-216), Hunan Science and Technology Innovation Plan (2025ZYJ003).

#### Disclosure of conflict of interest

None.

Address correspondence to: Dr. Yongjun Tan, State Key Laboratory of Chemo/Biosensing and Chemometrics, College of Biology, Hunan Research Center of the Basic Discipline for Cell Signaling, Hunan Engineering Research Center for Anticancer Targeted Protein Pharmaceuticals, Hunan University, Changsha 410082, Hunan, China. E-mail: yjtan@hnu.edu.cn

#### References

- [1] Sies H and Jones DP. Reactive oxygen species (ROS) as pleiotropic physiological signalling agents. Nat Rev Mol Cell Biol 2020; 21: 363-383
- [2] Srinivas US, Tan BWQ, Vellayappan BA and Jeyasekharan AD. ROS and the DNA damage response in cancer. Redox Biol 2019; 25: 101084.
- [3] Kennedy LJ, Moore K Jr, Caulfield JL, Tannenbaum SR and Dedon PC. Quantitation of 8-oxoguanine and strand breaks produced by four oxidizing agents. Chem Res Toxicol 1997; 10: 386-392.
- [4] Redza-Dutordoir M and Averill-Bates DA. Activation of apoptosis signalling pathways by reactive oxygen species. Biochim Biophys Acta 2016; 1863: 2977-2992.
- [5] Cooke MS, Evans MD, Dizdaroglu M and Lunec J. Oxidative DNA damage: mechanisms, mutation, and disease. FASEB J 2003; 17: 1195-1214.
- [6] Kuraoka I, Bender C, Romieu A, Cadet J, Wood RD and Lindahl T. Removal of oxygen free-radical-induced 5',8-purine cyclodeoxynucleosides from DNA by the nucleotide excision-re-

- pair pathway in human cells. Proc Natl Acad Sci U S A 2000; 97: 3832-3837.
- [7] Turrens JF. Mitochondrial formation of reactive oxygen species. J Physiol 2003; 552: 335-344.
- [8] Chio IIC and Tuveson DA. ROS in cancer: the burning question. Trends Mol Med 2017; 23: 411-429.
- [9] Harris IS and DeNicola GM. The complex interplay between antioxidants and ROS in cancer. Trends Cell Biol 2020; 30: 440-451.
- [10] Perkins A, Nelson KJ, Parsonage D, Poole LB and Karplus PA. Peroxiredoxins: guardians against oxidative stress and modulators of peroxide signaling. Trends Biochem Sci 2015; 40: 435-445.
- [11] Neumann CA, Cao J and Manevich Y. Peroxiredoxin 1 and its role in cell signaling. Cell Cycle 2009; 8: 4072-4078.
- [12] Rhee SG, Chae HZ and Kim K. Peroxiredoxins: a historical overview and speculative preview of novel mechanisms and emerging concepts in cell signaling. Free Radic Biol Med 2005; 38: 1543-1552.
- [13] Lennicke C and Cochemé HM. Redox metabolism: ROS as specific molecular regulators of cell signaling and function. Mol Cell 2021; 81: 3691-3707.
- [14] Marinho HS, Real C, Cyrne L, Soares H and Antunes F. Hydrogen peroxide sensing, signaling and regulation of transcription factors. Redox Biol 2014; 2: 535-562.
- [15] Guan X, Ruan Y, Che X and Feng W. Dual role of PRDX1 in redox-regulation and tumorigenesis: past and future. Free Radic Biol Med 2024; 210: 120-129.
- [16] Bajor M, Zych AO, Graczyk-Jarzynka A, Muchowicz A, Firczuk M, Trzeciak L, Gaj P, Domagala A, Siernicka M, Zagozdzon A, Siedlecki P, Kniotek M, O'Leary PC, Golab J and Zagozdzon R. Targeting peroxiredoxin 1 impairs growth of breast cancer cells and potently sensitises these cells to prooxidant agents. Br J Cancer 2018; 119: 873-884.
- [17] Chen Q, Li J, Yang X, Ma J, Gong F and Liu Y. Prdx1 promotes the loss of primary cilia in esophageal squamous cell carcinoma. BMC Cancer 2020; 20: 372.
- [18] Herman L, Todeschini AL and Veitia RA. Fork-head transcription factors in health and disease. Trends Genet 2021; 37: 460-475.
- [19] O'Regan RM and Nahta R. Targeting forkhead box M1 transcription factor in breast cancer. Biochem Pharmacol 2018; 154: 407-413.
- [20] Liang SK, Hsu CC, Song HL, Huang YC, Kuo CW, Yao X, Li CC, Yang HC, Hung YL, Chao SY, Wu SC, Tsai FR, Chen JK, Liao WN, Cheng SC, Tsou TC and Wang IC. FOXM1 is required for small cell lung cancer tumorigenesis and associated

- with poor clinical prognosis. Oncogene 2021; 40: 4847-4858.
- [21] Kalathil D, John S and Nair AS. FOXM1 and cancer: faulty cellular signaling derails homeostasis. Front Oncol 2020; 10: 626836.
- [22] Wang X, Kiyokawa H, Dennewitz MB and Costa RH. The forkhead box m1b transcription factor is essential for hepatocyte DNA replication and mitosis during mouse liver regeneration. Proc Natl Acad Sci U S A 2002; 99: 16881-16886.
- [23] Yang C, Chen H, Tan G, Gao W, Cheng L, Jiang X, Yu L and Tan Y. FOXM1 promotes the epithelial to mesenchymal transition by stimulating the transcription of Slug in human breast cancer. Cancer Lett 2013; 340: 104-112.
- [24] Gemenetzidis E, Elena-Costea D, Parkinson EK, Waseem A, Wan H and Teh MT. Induction of human epithelial stem/progenitor expansion by FOXM1. Cancer Res 2010; 70: 9515-9526
- [25] Li SK, Smith DK, Leung WY, Cheung AM, Lam EW, Dimri GP and Yao KM. FoxM1c counteracts oxidative stress-induced senescence and stimulates Bmi-1 expression. J Biol Chem 2008; 283: 16545-16553.
- [26] Park HJ, Carr JR, Wang Z, Nogueira V, Hay N, Tyner AL, Lau LF, Costa RH and Raychaudhuri P. FoxM1, a critical regulator of oxidative stress during oncogenesis. EMBO J 2009; 28: 2908-2918.
- [27] Tan Y, Raychaudhuri P and Costa RH. Chk2 mediates stabilization of the FoxM1 transcription factor to stimulate expression of DNA repair genes. Mol Cell Biol 2007; 27: 1007-1016.
- [28] Horton JK, Watson M, Stefanick DF, Shaughnessy DT, Taylor JA and Wilson SH. XRCC1 and DNA polymerase beta in cellular protection against cytotoxic DNA single-strand breaks. Cell Res 2008; 18: 48-63.
- [29] Bu H, Lan X, Cheng H, Pei C, Ouyang M, Chen Y, Huang X, Yu L and Tan Y. Development of an interfering peptide M1-20 with potent anticancer effects by targeting FOXM1. Cell Death Dis 2023; 14: 533.
- [30] Xiang Q, Tan G, Jiang X, Wu K, Tan W and Tan Y. Suppression of FOXM1 transcriptional activities via a single-stranded DNA aptamer generated by SELEX. Sci Rep 2017; 7: 45377.
- [31] Zhang Y, Ding N, Li Y, Ouyang M, Fu P, Peng Y and Tan Y. Transcription factor FOXM1 specifies chromatin DNA to extracellular vesicles. Autophagy 2024; 20: 1054-1071.
- [32] Lee SR, Yang KS, Kwon J, Lee C, Jeong W and Rhee SG. Reversible inactivation of the tumor suppressor PTEN by H2O2. J Biol Chem 2002; 277: 20336-20342.
- [33] Sobotta MC, Liou W, Stöcker S, Talwar D, Oehler M, Ruppert T, Scharf AN and Dick TP. Peroxiredoxin-2 and STAT3 form a redox relay

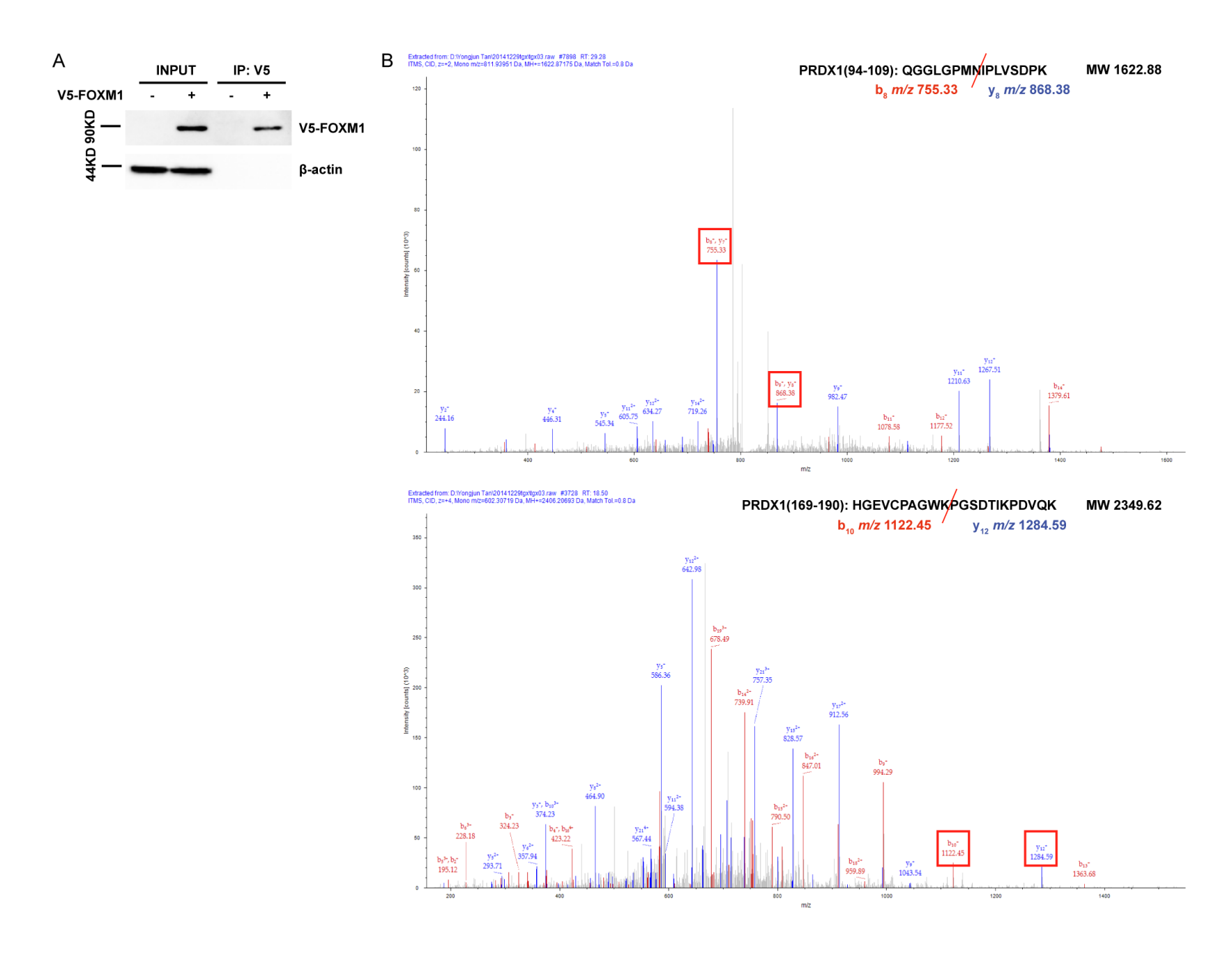
- for H202 signaling. Nat Chem Biol 2015; 11: 64-70.
- [34] Bolduc J, Koruza K, Luo T, Malo Pueyo J, Vo TN, Ezerina D and Messens J. Peroxiredoxins wear many hats: factors that fashion their peroxide sensing personalities. Redox Biol 2021; 42: 101959.
- [35] Watson WH, Pohl J, Montfort WR, Stuchlik O, Reed MS, Powis G and Jones DP. Redox potential of human thioredoxin 1 and identification of a second dithiol/disulfide motif. J Biol Chem 2003; 278: 33408-33415.
- [36] Su X, Yang Y, Yang Q, Pang B, Sun S, Wang Y, Qiao Q, Guo C, Liu H and Pang Q. NOX4-derived ROS-induced overexpression of FOXM1 regulates aerobic glycolysis in glioblastoma. BMC Cancer 2021; 21: 1181.
- [37] Paull TT, Rogakou EP, Yamazaki V, Kirchgessner CU, Gellert M and Bonner WM. A critical role for histone H2AX in recruitment of repair factors to nuclear foci after DNA damage. Curr Biol 2000; 10: 886-895.
- [38] Ledgerwood EC, Marshall JW and Weijman JF. The role of peroxiredoxin 1 in redox sensing and transducing. Arch Biochem Biophys 2017; 617: 60-67.
- [39] Dalle-Donne I, Rossi R, Colombo R, Giustarini D and Milzani A. Biomarkers of oxidative damage in human disease. Clin Chem 2006; 52: 601-623.
- [40] Isola JJ, Helin HJ, Helle MJ and Kallioniemi OP. Evaluation of cell proliferation in breast carcinoma. Comparison of Ki-67 immunohistochemical study, DNA flow cytometric analysis, and mitotic count. Cancer 1990; 65: 1180-1184.
- [41] Kopanja D, Chand V, O'Brien E, Mukhopadhyay NK, Zappia MP, Islam ABMMK, Frolov MV, Merrill BJ and Raychaudhuri P. Transcriptional repression by FoxM1 Suppresses tumor differentiation and promotes metastasis of breast cancer. Cancer Res 2022; 82: 2458-2471.
- [42] Wei P, Zhang N, Wang Y, Li D, Wang L, Sun X, Shen C, Yang Y, Zhou X and Du X. FOXM1 promotes lung adenocarcinoma invasion and metastasis by upregulating SNAIL. Int J Biol Sci 2015; 11: 186-198.
- [43] Kim JH, Bogner PN, Baek SH, Ramnath N, Liang P, Kim HR, Andrews C and Park YM. Upregulation of peroxiredoxin 1 in lung cancer and its implication as a prognostic and therapeutic target. Clin Cancer Res 2008; 14: 2326-2333.
- [44] Sun HN, Ma DY, Guo XY, Hao YY, Jin MH, Han YH, Jin X and Kwon T. Peroxiredoxin I and II as novel therapeutic molecular targets in cervical cancer treatment through regulation of endoplasmic reticulum stress induced by bleomycin. Cell Death Discov 2024; 10: 267.

- [45] Cook KM and Hogg PJ. Post-translational control of protein function by disulfide bond cleavage. Antioxid Redox Signal 2013; 18: 1987-2015
- [46] Alegre-Cebollada J, Kosuri P, Rivas-Pardo JA and Fernández JM. Direct observation of disulfide isomerization in a single protein. Nat Chem 2011; 3: 882-887.
- [47] Maag D, Putzu M, Gómez-Flores CL, Gräter F, Elstner M and Kubař T. Electrostatic interactions contribute to the control of intramolecular thiol-disulfide isomerization in a protein. Phys Chem Chem Phys 2021; 23: 26366-26375.
- [48] Laoukili J, Alvarez M, Meijer LA, Stahl M, Mohammed S, Kleij L, Heck AJ and Medema RH. Activation of FoxM1 during G2 requires cyclin A/Cdk-dependent relief of autorepression by the FoxM1 N-terminal domain. Mol Cell Biol 2008; 28: 3076-3087.
- [49] Balsera M and Buchanan BB. Evolution of the thioredoxin system as a step enabling adaptation to oxidative stress. Free Radic Biol Med 2019; 140: 28-35.
- [50] Kim SY, Kim TJ and Lee KY. A novel function of peroxiredoxin 1 (Prx-1) in apoptosis signal-regulating kinase 1 (ASK1)-mediated signaling pathway. FEBS Lett 2008; 582: 1913-1918.
- [51] Saitoh M, Nishitoh H, Fujii M, Takeda K, Tobiume K, Sawada Y, Kawabata M, Miyazono K and Ichijo H. Mammalian thioredoxin is a direct inhibitor of apoptosis signal-regulating kinase (ASK) 1. EMBO J 1998; 17: 2596-2606.
- [52] Kylarova S, Kosek D, Petrvalska O, Psenakova K, Man P, Vecer J, Herman P, Obsilova V and Obsil T. Cysteine residues mediate high-affinity binding of thioredoxin to ASK1. FEBS J 2016; 283: 3821-3838.
- [53] Cao Z and Lindsay JG. The peroxiredoxin family: an unfolding story. Subcell Biochem 2017; 83: 127-147.
- [54] Wood ZA, Poole LB and Karplus PA. Peroxiredoxin evolution and the regulation of hydrogen peroxide signaling. Science 2003; 300: 650-653
- [55] Yan Y, Wladyka C, Fujii J and Sockanathan S. Prdx4 is a compartment-specific H2O2 sensor that regulates neurogenesis by controlling surface expression of GDE2. Nat Commun 2015; 6: 7006.
- [56] Lipinski S, Pfeuffer S, Arnold P, Treitz C, Aden K, Ebsen H, Falk-Paulsen M, Gisch N, Fazio A, Kuiper J, Luzius A, Billmann-Born S, Schreiber S, Nuñez G, Beer HD, Strowig T, Lamkanfi M, Tholey A and Rosenstiel P. Prdx4 limits caspase-1 activation and restricts inflammasomemediated signaling by extracellular vesicles. EMBO J 2019; 38: e101266.

# The oxidative modification of FOXM1

**Table S1.** Sequences of primers for constructing point mutation in plasmids

Name	S: 5'-3'	AS: 5'-3'
PRDX1 C52S	TTG TGA GCC CCA CGG AGA TCA TTG	CGT GGG GCT CAC AAA GGT GAA GTC
PRDX1 C173S	AAG TGA GCC CAG CTG GCT GGA AAC	GCT GGG CTC ACT TCC CCA TGT TTG
FOXM1 C160A	CCC TTG CCG AGC AGA AAC GGG AGA C	TGC TCG GCA AGG GCT CCA GGT GGT
FOXM1 C167A	GGA GAC GCT GCA GAT GGT GAG GCA	ACC ATC TGC AGC GGT CTC CCG TTT CTG
FOXM1 C175A	AGC AGG CGC CAC TAT CAA CAA TAG CCT	ATA GTG GCG CCT GCT GCC TCA CCA T
FOXM1 C511A	AAC CCG GGC TGT CTC GGA AAT GCT TGT	GAG ACA GCC CGG GTT GGG GAC CTA
FOXM1 C539A	CTC CCG CTG TGG ATG AGC CGG AG	ATC CAC AGC GGG AGG CAG TAG ATG CT
TRX1 C32S	CGT GGT CTG GGC CTT GCA AAA TGA	GGC CCA GAC CAC GTG GCT GAG AAG
TRX1 C35S	GGC CTA GCA AAA TGA TCA AGC CTT TC	CAT TTT GCT AGG CCC ACA CCA CGT



# The oxidative modification of FOXM1

**Figure S1.** The identification of FOXM1-interacting proteins by MS. (A) HEK293T cells were transfected with pC-MV-V5-FOXM1. Cell lysates were immunoprecipitated with anti-V5 antibody and protein A/G agarose beads, and blotted by anti-V5 antibodies. Ten percent of cell lysates were used as input control. (B) After trypsin digestion, the samples produced from (A) were analyzed by MS and the identified PRDX1 peptides from MS were showed.

Table S2. The selected FOXM1-interacting proteins identified by MS

Accession	Description	Score
Q13162	Peroxiredoxin-4 OS=Homo sapiens GN=PRDX4 PE=1 SV=1 - [PRDX4_HUMAN]	10.28
Q06830	Peroxiredoxin-1 OS=Homo sapiens GN=PRDX1 PE=1 SV=1 - [PRDX1_HUMAN]	7.83
A6NIW5	Peroxiredoxin 2, isoform CRA_a OS=Homo sapiens GN=PRDX2 PE=1 SV=2 - [A6NIW5_HUMAN]	2.95
P10599	Thioredoxin OS=Homo sapiens GN=TXN PE=1 SV=3 - [THIO_HUMAN]	3.24

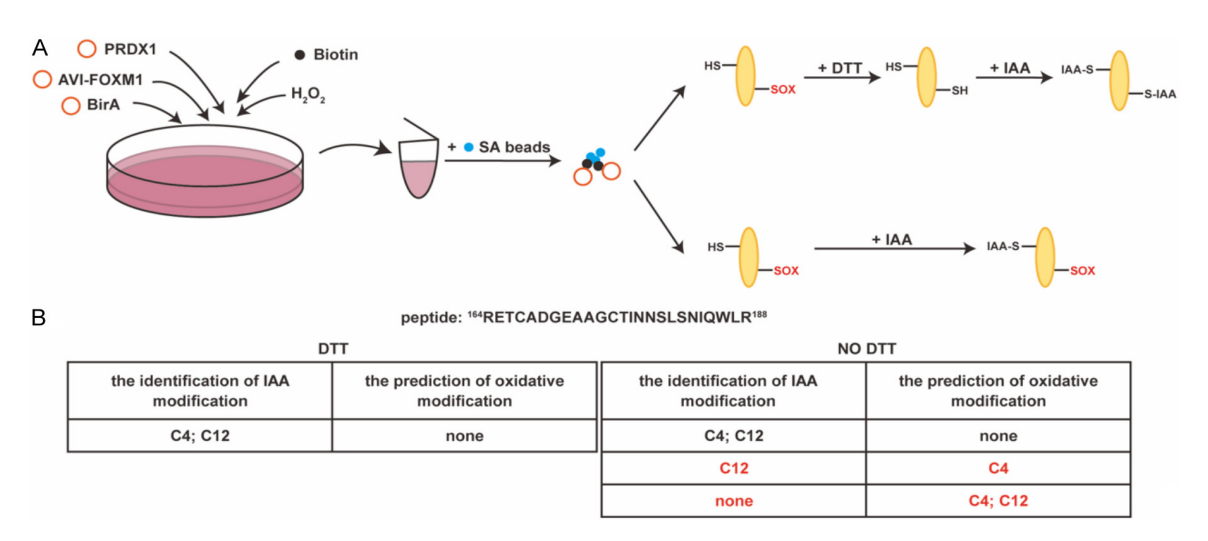
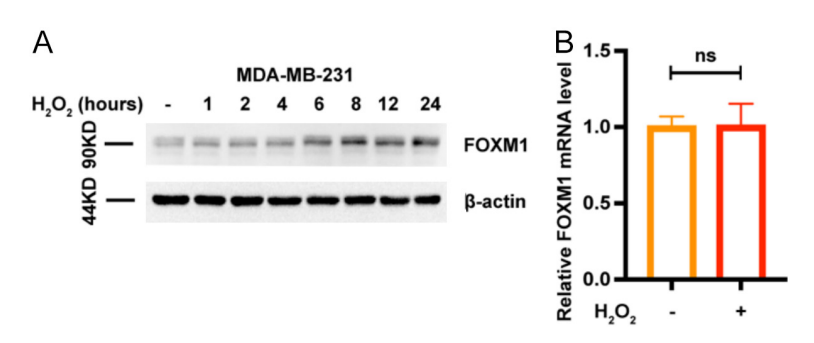


Figure S2. The identification of redox sensitive cysteines in FOXM1 by MS. (A) HEK293T cells were transfected with pEF1-BirA, pCMV-AVI-FOXM1 and pCMV-PRDX1 and treated with  ${\rm H_2O_2}$  (50  ${\rm \mu M}$ ) for 2 min before harvesting. Before transfection, Biotin were added into cell culture medium. Cell lysates were immunoprecipitated with anti-Streptavidin (SA) agarose beads, then protein samples were eluted from beads and separated equally into two groups. After been treated with DTT and IAA, and digested by trypsin, samples were detected by mass spectrometer. (B) The identification of intramolecular disulfide bond in the oxidized FOXM1. Samples were produced as procedures in (A) and the identified FOXM1 peptides from MS were showed. The FOXM1 C167 and C175 were not modified by IAA in No DTT group but modified by IAA in DTT group.



**Figure S3.** The protein levels of FOXM1 were increased by  ${\rm H_2O_2}$  treatment in MDA-MB-231 cells. A. MDA-MB-231 cells were seeded in a 12-well plate and cultured for 48 h and treated with  ${\rm H_2O_2}$  (200  $\mu$ M) by a concentration gradient (1, 2, 4, 6, 8, 12 or 24 h) before harvesting. The FOXM1 proteins were blotted by anti-FOXM1 antibodies. B. MDA-MB-231 cells were treated with  ${\rm H_2O_2}$  (200  $\mu$ M) for 24 h, and then RNAs were extracted. The mRNA levels of FOXM1 were detected by qPCR and normalized to the GAPDH. n = 3, ns, P > 0.05; two-tailed unpaired Student's t-test.

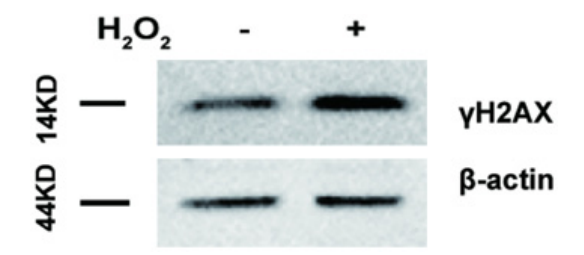
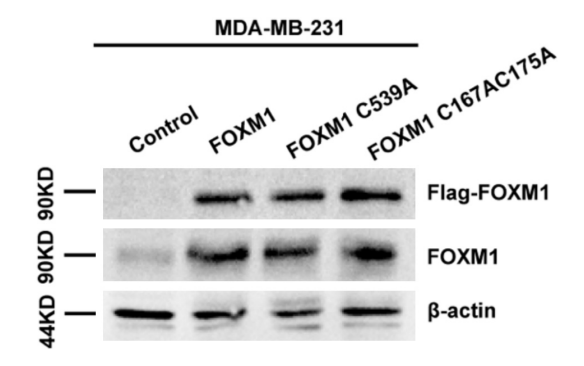
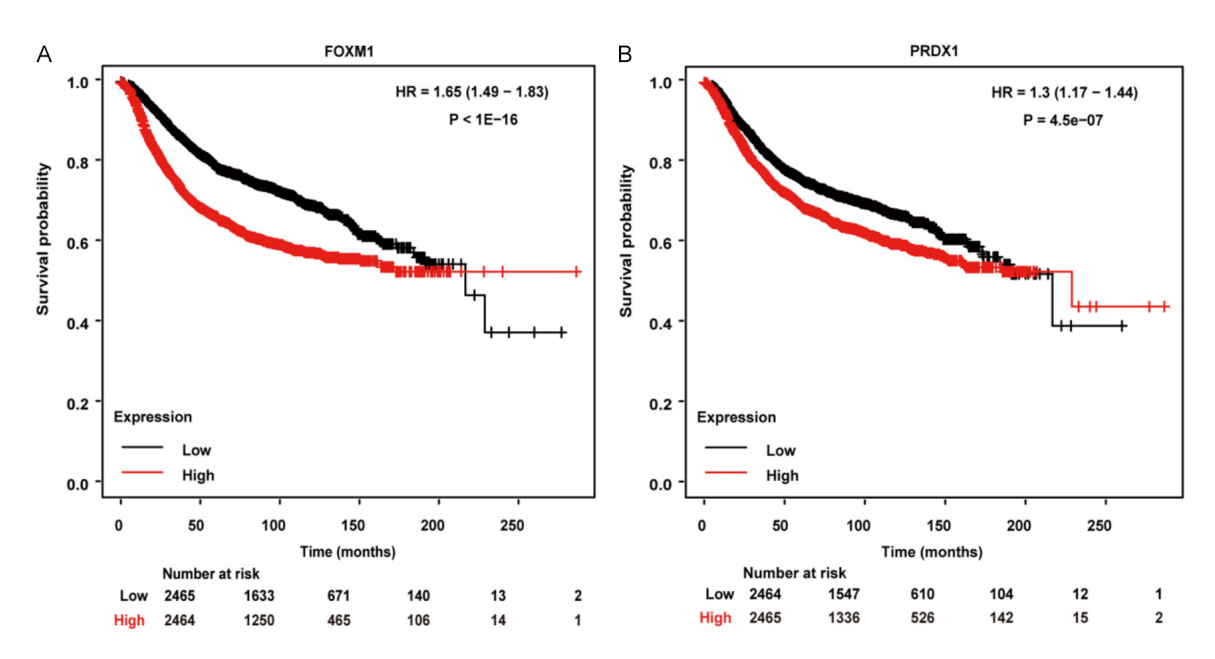


Figure S4. The DNA damage increased with  $\rm H_2O_2$  treatment in HEK293T cells. HEK293T cells were treated with  $\rm H_2O_2$  (200  $\mu$ M) for 24 h before harvesting. The proteins of  $\rm \gamma H2AX$  were blotted by anti- $\rm \gamma H2AX$  antibodies.



**Figure S5.** The exogenous and endogenous FOXM1 levels in MDA-MB-231<sup>control</sup>, MDA-MB-231<sup>FOXM1</sup>, MDA-MB-231<sup>FOXM1</sup>, MDA-MB-231<sup>FOXM1</sup> and MDA-MB-231<sup>FOXM1</sup> cell lines. After puromycin selection, MDA-MB-231<sup>Control</sup>, MDA-MB-231<sup>FOXM1</sup>, MDA-MB-231<sup>FOXM1</sup> cells were harvested. The protein levels of Flag-FOXM1 and endogenous FOXM1 in cell lysates were blotted by anti-Flag and anti-FOXM1 antibodies.



**Figure S6.** The high levels of FOXM1 or PRDX1 were associated with poor survival probability in breast cancer patients. The FOXM1-related survival probability and PRDX1-related survival probability in breast cancer patients (TCGA database, n=4929) were analyzed from Kmplot website (https://kmplot.com/analysis). The mean value was set as the cut-off value to separate high or low expression.

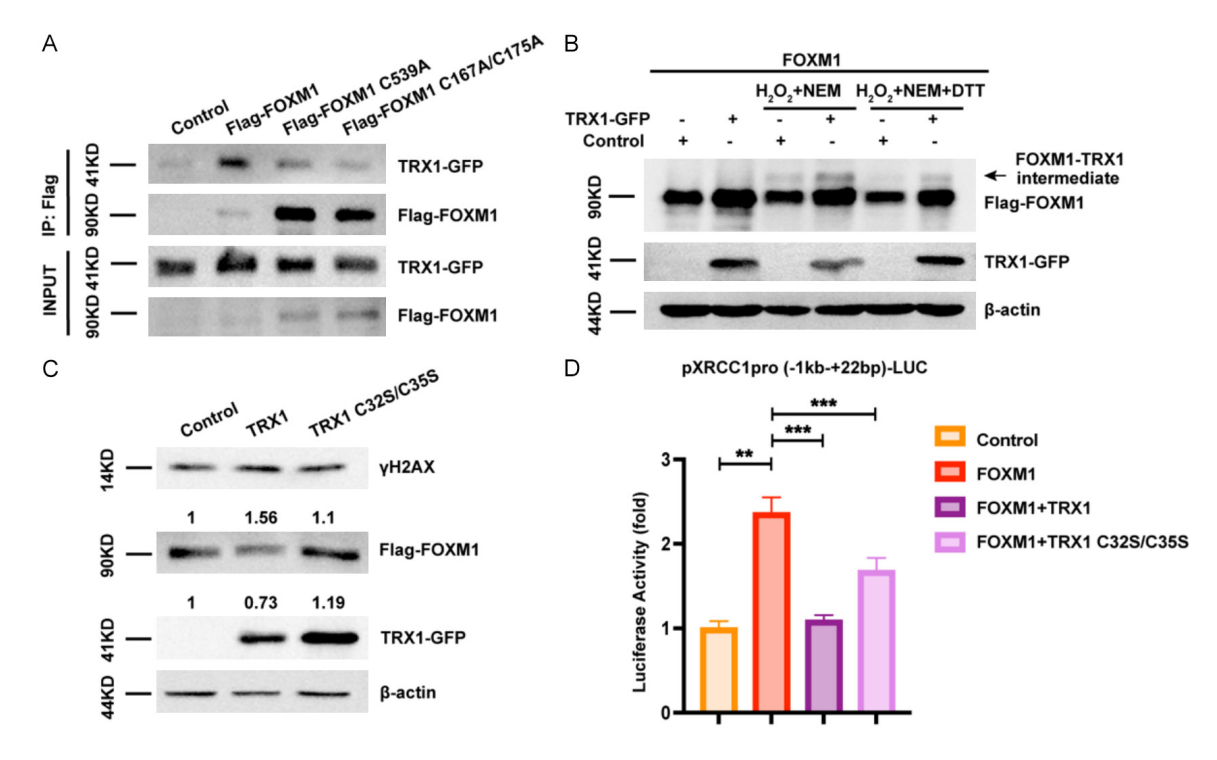
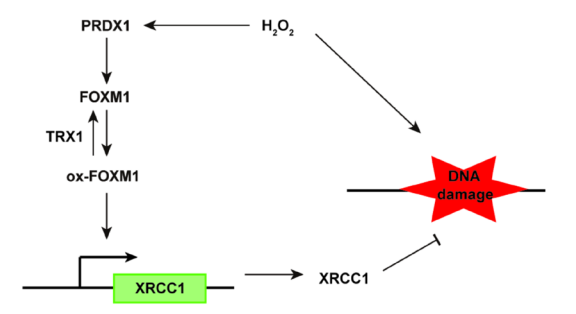


Figure S7. FOXM1 interacted with TRX1. A. HEK293T cells were transfected with pCMV-Flag-FOXM1, pCMV-Flag-FOXM1 C539A or pCMV-Flag-FOXM1 C167A/C175A together with pcDNA3.1-TRX1-GFP. Cell lysates were incubated with anti-Flag agarose beads and blotted by anti-Flag and anti-GFP antibodies. Ten percent of cell lysates were used as input control. B. HEK293T cells were transfected with pCMV-Flag-FOXM1 and pCMV-TRX1-GFP, cells were treated with  ${\rm H_2O_2}$  (200  ${\rm \mu M}$ ) for 7.5 min and then treated with NEM (100 mM) for 5 min before harvesting. Control samples were treated with additional DTT (50 mM) for 5 min. The protein of FOXM1 and TRX1 were detected by non-reducing Western blotting with anti-Flag and anti-GFP antibodies. The arrow indicated the intermediate of FOXM1-TRX1. C. HEK293T cells were transfected with pCMV-TRX1-GFP or pCMV-TRX1 C32S/C35S-GFP, plus pCMV-Flag-FOXM1 and treated with  ${\rm H_2O_2}$  (200  ${\rm \mu M}$ ) for 24 h before harvesting. The proteins of  ${\rm YH2AX}$ , FOXM1 and TRX1 in cell lysates were blotted by anti-YH2AX, anti-Flag and anti-GFP antibodies. D. HEK293T cells were transfected with pRL-CMV, pXRC-C1pro (-1kb-+22bp)-LUC, pCMV-Flag-FOXM1 together with pCMV-TRX1-GFP or pCMV-TRX1 C32S/C35S-GFP and treated with  ${\rm H_2O_2}$  (200  ${\rm \mu M}$ ) for 24 h before harvesting. Then cell lysates were collected to measure the luciferase activities. n = 3, \*\*, P < 0.01; \*\*\*, P < 0.001; two-tailed unpaired Student's t-test.



**Figure S8.** A schematic illustrating that PRDX1-mediated FOXM1 oxidation activated the expression of XRCC1 gene to repair DNA damage. H<sub>2</sub>O<sub>2</sub>-induced oxidative stress caused DNA damage and the oxidation of PRDX1, which oxidized FOXM1 to stimulate the expression of DNA damage repair gene XRCC1 to prevent DNA damage. TRX1 could reduce the oxidized FOXM1 and resulted in the redox cycle of FOXM1 protein.